JOURNAL OF ENGINEERING RESEARCH & SCIENCES

JENRS

Editorial

In this edition, we explore diverse advancements in technology and environmental sciences, focusing on semiconductor fabrication, bioplastics, housing security systems, and quantum-enhanced machine learning for remote sensing. These research papers present innovative solutions to current challenges and provide insights into the future directions of these fields.

The first paper addresses the contamination issues by halogens (such as F, Cl, and Br) in semiconductor wafer fabrication, specifically in the back end of line (BEOL) processes. These contaminants cause significant challenges in metallization, leading to severe metal corrosion and defects in aluminum (Al) metal lines, bond pads, and vias. The study presents a detailed failure analysis of worm-like defects caused by Cl contamination, proposing a corrosion mechanism where a Cl-based chemical chain reaction leads to continuous and enhanced chemical corrosion. This research underscores the importance of addressing contamination issues to improve yield and reliability in semiconductor manufacturing [1].

The second paper focuses on the production of bioplastics as a sustainable alternative to conventional plastics. The study isolates and optimizes bacteria capable of producing bioplastics using sawdust, an agro-waste, as a low-cost substrate. Among the isolates, Bacillus cereus-SD2 showed the highest bioplastic (PHB) production under optimized growth conditions. This research highlights the potential of using waste materials and bacterial fermentation to produce environmentally friendly bioplastics, suggesting further optimization for industrial-scale production [2].

The third paper addresses the need for enhanced security systems in housing societies, particularly in the context of the COVID-19 pandemic. The proposed solution integrates facial recognition with body temperature sensing on a Raspberry Pi, coupled with an automated data collection web application. This system aims to improve safety and monitoring in housing societies, demonstrating the potential of combining biometric data with health monitoring technologies to address current public health challenges [3].

The fourth paper explores the application of quantum-enhanced machine learning for binary classification of satellite remote sensing data. The study compares the performance of a Support Vector Machine-quantum annealing solver (SVM-QA) with classical machine learning algorithms using 16 pre-labeled datasets. The results indicate that in 10 out of 16 datasets, the SVM-QA classifier outperforms classical algorithms in classification accuracy. This research suggests that quantum computing can significantly enhance remote sensing data analysis, contributing to more accurate environmental monitoring and decision-making [4].

These featured research papers highlight the innovative approaches being developed to tackle challenges in various fields, from semiconductor manufacturing and bioplastic production to housing security and remote sensing. Each study provides valuable insights and practical solutions that can drive future advancements and applications.

References:

[1]   H. Younan, L.J. Lois, L. Binghai, Z. Lei, L. Xiaomin, "Failure Analysis & Mechanism Studies of the Worm-like Defects in Vias of Wafer Fabrication," Journal of Engineering Research and Sciences, vol. 2, no. 12, pp. 1–6, 2023, doi:10.55708/js0212001.

[2]   A. Javaid, S. Aslam, H. Qaisar, F. Batool, R. Javed, M.W. Qaisar, "Isolation and Characterization of the Bioplastic Producing Bacteria Using Low-Cost Substrate, Sawdust," Journal of Engineering Research and Sciences, vol. 2, no. 12, pp. 7–14, 2023, doi:10.55708/js0212002.

[3]   N. Koppikar, N. Koppikar, "Smart Monitoring System for Housing Societies based on Deep Learning and IoT," Journal of Engineering Research and Sciences, vol. 2, no. 12, pp. 15–22, 2023, doi:10.55708/js0212003.

[4]   Y. Liu, W. Wang, H. Wang, B. Alidaee, "Quantum Machine Learning on Remote Sensing Data Classification," Journal of Engineering Research and Sciences, vol. 2, no. 12, pp. 23–33, 2023, doi:10.55708/js0212004.

Editor-in-chief

Prof. Paul Andrew

JOURNAL OF ENGINEERING RESEARCH AND SCIENCES

CONTENTS

Failure Analysis & Mechanism Studies of the Worm-like Defects in Vias of Wafer Fabrication

Hua Younan*, **Liao Jinzhi Lois, Liu Binghai, Zhu Lei, Li Xiaomin**

WinTech Nano-Technology Services Pte. Ltd.,10 Science Park Road, #03-26, The Alpha Science Park II, Singapore 117684
*Corresponding author: Hua Younan, email: younan@wintech-nano.com

ABSTRACT: In semiconductor wafer fabrication, the contamination issue by halogens (such as F, Cl, and Br) brings great challenges to metallization processes in the back end of line (BEOL). For aluminum (Al) back-end process, severe metal corrosion may occur by halogens, forming aluminum halide defects. Such halogen-induced metal corrosion issue creates the defects on Al metal lines, Al bondpads and Vias, causing direct device failure, resulting in low yield and reliability issue. In this paper, we reported failure analysis and mechanism studies of the Worm-like defects in Via holes, which was caused by Cl contamination and the subsequent Al metal corrosion. With this study, a corrosion mechanism was proposed in which a Cl-based chemical chain-reaction resulted in repeated/continuously enhanced chemical corrosion even with a small amount of Cl ions. The chemical chain-reactions caused more serious corrosion with corrosive by-products. Such Cl-induced Al metal corrosion and the worm-like defect formation resulted in the process integrity issues related to Al metallization processes, such as voiding in Via structures, opening or bridging in between metal lines.

KEYWORDS: failure analysis, Cl corrosion, the Worm-like defects, Vias and wafer fabrication

1. Introduction

In semiconductor wafer fabrication, the contamination issue by halogens (such as F, Cl, and Br) brings great challenges to metallization processes in the back end of line (BEOL). Table 1 indicates the typical plasma etch gases used for each type of material in wafer fabrication (fab), which may cause Cl, F and Br cross contamination [1].

Table 1: Typical plasma etch gases for polysilicon, SiO_2 and Al films

Material	Etchant
Polysilicon	CF_4
	CF_4/H_2
	CF_4/O_2, SF_6
	HBr, Cl_2, $Cl_2/HBr/O_2$
SiO_2	SF_6, NF_3, CF_4/O_2, CF_4
Al	Cl_2
	$Cl_2/CHCl_3$, Cl_2/N_2

For aluminum (Al) back-end process, severe metal corrosion may occur by halogens, forming aluminum halide defects. Such halogen-induced metal corrosion issue creates the defect on Al metal lines, Al bondpads and Vias, causing direct device failure, resulting in low yield and reliability issue.

In our previous papers, we have performed failure analysis and mechanism studies on fluorine (F) contamination and their Al halide defects. We have presented detailed studies on the failure mechanisms and failure models, and proposed corrective and preventive measures, as well as process monitoring solutions which are useful in semiconductor industries and wafer fab [2-5].

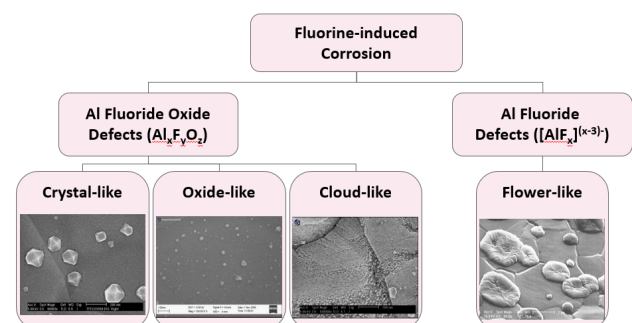Figure 1: The F-induced corrosion defects were classified as the "flower-like", "crystal-like", "oxide-like" and "cloud-like" defects.

For example, we have deeply studied the F-induced corrosion defects and proposed the related failure models, and made classification for the F-induced corrosion defects on the Al bondpads as the "flower-like", "crystal-like", "oxide-like" and "cloud-like" defects as shown in

Figure 1, which have been characterized using SEM/EDX, TEM, Auger, XPS and TOF-SIMS analysis techniques [4].

In this paper, we will perform failure analysis and mechanism studies of the Cl-induced defects, especially for the Worm-like defects in Via holes after Via etching process in wafer fab, which is caused by chlorine (Cl) contamination and corrosion in wafer fab during Via processes.

2. Cl-Induced Corrosion and Failure Analysis of the Worm-Like Defects in Via Holes

In wafer fab, the control of Cl contamination in production should be very strict as it will result in severe metal Cl corrosion. Cl contamination and the formation of corrosion defects is prone to occur in Al metallization and Vias forming processes, because Cl-containing gases (such as Cl_2, $CHCl_3$, BCl_3, etc.) are used in Al metallization BEOL processes in wafer fab. After fab processes, certain amount of Cl may not be completely cleaned away, leaving behind the corrosive Cl-containing residue or contaminants although the cleaning processes are employed after metal etching process. Moreover, sometime, Cl contamination may be from wafer fab environment or/and from the mini-environment of SMIF pods, which is used to transport.

2.1. Cl Contamination and Corrosion

Once Cl contamination occurs in wafer fab, Cl will chemically react with Al to form Al chloride. Its typical chemical reaction formula is:

$$Al + 3Cl- \rightarrow AlCl_3 + 3e- \qquad (1)$$

(Water soluble)
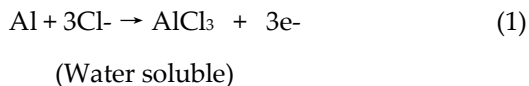
Based on our study results and the associated Cl-based chemistry, the chemical reactions and corrosion between Cl and Al metal are very fast and intensive ones, unlike those chemical corrosion induced by F contaminant in which the initiation of F-based corrosion may need certain period of time, e.g., hours usually.
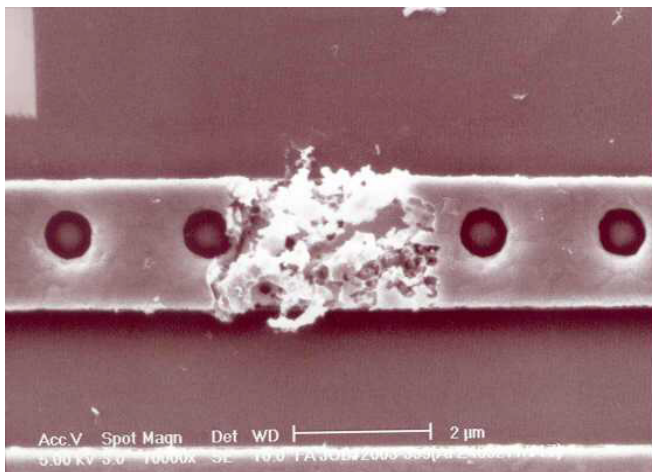

Figure 2: SEM micrograph showed the corrosive defect on Al metal line due to Cl-induced corrosion.

Figure 2 shows a Cl corrosive defect on the Al metal line. One can see that the defect has damaged the metal line, which may cause low yield or reliability issue. The root cause was identified to be Cl environment contamination. It is understood that differencing from F-induced corrosion, Cl-induced corrosion is immediate. Moreover, $AlCl_3$ is a chemically unstable compound and it dissolves in water. Therefore, Cl-induced corrosion is more serious as it can cause chemical chain reactions (see discussion in the next session).

2.2. The Worm-like Defects in Al Via Holes

As all we know, in typical Al-based BEOL processes, W Vias structures serve as the interconnects in between different Al metal layers, as shown in Figure 3. The formation of W vias involved somewhat complicated process sequences, from the initial Al metal line patterning, to IMD CVD processes, to via hole etch and etch, barrier-layer deposition and W filling, and to the final W CMP processes. Any issue related to the integrity of the above-mentioned processes may lead to the direct device failure, causing low yield and reliability failure.

In this case, we reported an interesting case study related to Cl contamination and the associated Al metal corrosion, i.e., the worm-like defect formation after Via hole etching process in wafer fab.
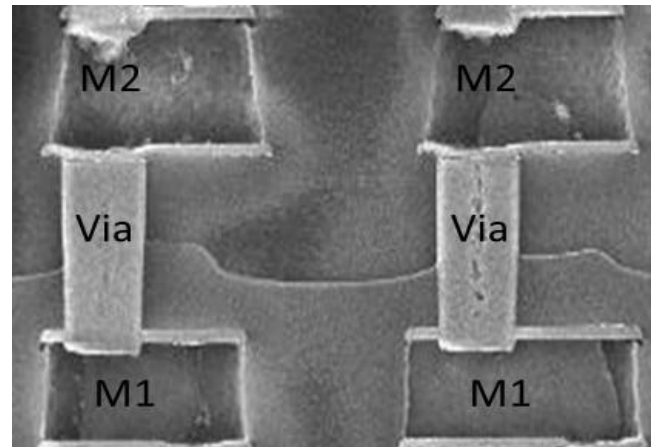
Figure 3: A typical metal via connection, two via-1s formed the inter-connect in between M1 and M2 metal lines.

In this case, we reported an interesting case study related to Cl contamination and the associated Al metal corrosion, i.e., the worm-like defect formation after Via hole etching process in wafer fab.

Inline SEM inspection after VIA hole etch process revealed the formation of bountiful worm-like defects, protruding from via holes, as shown by the SEM images in Figure 4. With the presence of these worm-like defects will definitely affect the subsequent processes like deposition of the barrier layers and W layer. In order to the understand the root-cause behind the formation worm-like defects, we performed detailed failure analysis and failure mechanism studies.
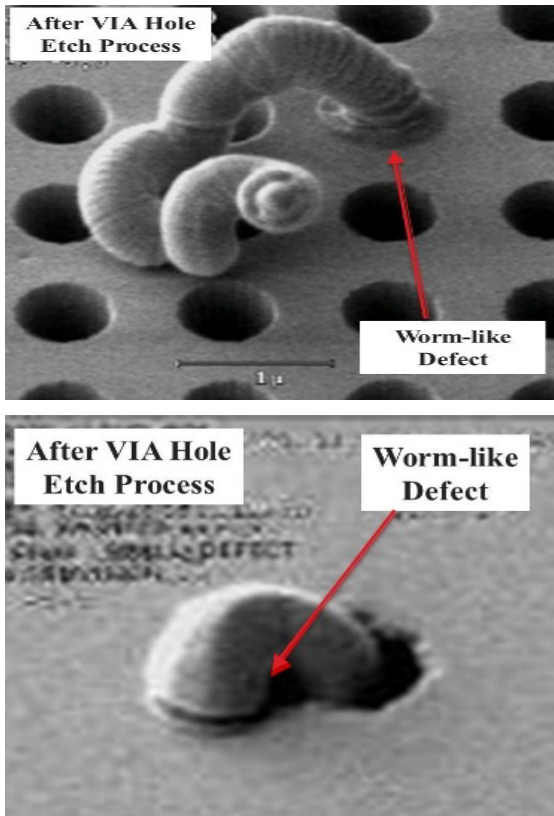
Figure 4: The Worm-like defects were found in Via holes after Via hole etching processes in wafer fab. At the bottom of the via holes, it was Al M1.

3. Failure analysis and mechanism studies of the worm-like defects in via holes

Figure 5 shows the micro-area EDX analysis on the worm-like defect. As shown in Figure 5, a small amount of Cl was detected, indicating that the worm-like defect was formed due to Cl-induced corrosion. Further FIB-SEM analysis showed that the worm-like defects directly grew from the bottom Al M1 layer along the via holes.

Figure 5: EDX on the Worm-like defect detected Cl peak and confirmed that it was Cl-induced corrosion defect.

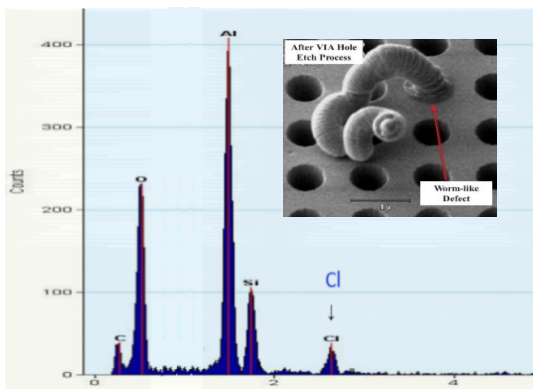Nonetheless, it was still difficult to understand how these Cl-corrosion worm-like defects were so intensive that the corrosion-induced by products were able to protrude from the bottom M1 to top via hole surface with long tails. Here, in term of Cl-based chemistry, we proposed the Cl chain chemical reactions theory and these worm-like defects were not due to simple chemical

corrosion reaction, but due to the Cl chain chemical reactions, where only a small amount of Cl ions could propagate in chemical reactions repeatedly, and finally it causes very intensive Cl corrosion reactions even with a small amount of Cl ions.

3.1. Failure Mechanism

After performing studies, we have understood that:

a) Cl-corrosion is self-sustained;

b) A small amount of Cl ions is sufficient to trigger the corrosion;

c) Cl and Al form Al chloride ($AlCl_3$) which is water-soluble.

Cl contamination chemically reacts with Al to form $AlCl_3$ as Eqn (1), which is a chemically unstable compound and it is water soluble. Therefore, $AlCl_3$ can further chemically react with water or moisture (H_2O) and form hydrated Aluminium hydroxide product ($Al(OH)_3$) and further release Cl^- ions:

$$AlCl_3 + 3\ H_2O \rightarrow Al(OH)_3 + 3Cl^- + 3H^+ \qquad (2)$$
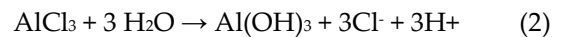
The new product of hydrated Aluminium hydroxide product ($Al(OH)_3$) will be discomposed and forms Al oxide (Al_2O_3):
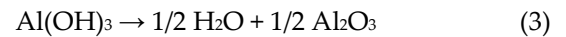
$$Al(OH)_3 \rightarrow 1/2\ H_2O + 1/2\ Al_2O_3 \qquad (3)$$

Because $AlCl_3$ is water-soluble, it can release Cl ions again when it encounters water vapor, and further corrodes Al metal. Therefore, a small amount of Cl ions could repeatedly propagate in chemical reactions, causing a Cl chain chemical reaction, which produces alumina, a corrosion product:

$$+6\ H_2O$$

$$2Al + 6Cl^- \rightarrow 2AlCl_3 \quad \rightarrow \quad 2Al(OH)_3 + 6Cl^- + 6H^+$$

$$-3H2O$$

$$Al_2O_3 \qquad (4)$$

$$nAl_2O_3 + mAlCl_3 \rightarrow Al_xCl_yO_z \ \ \text{(Worm-like defects)} \ (5)$$
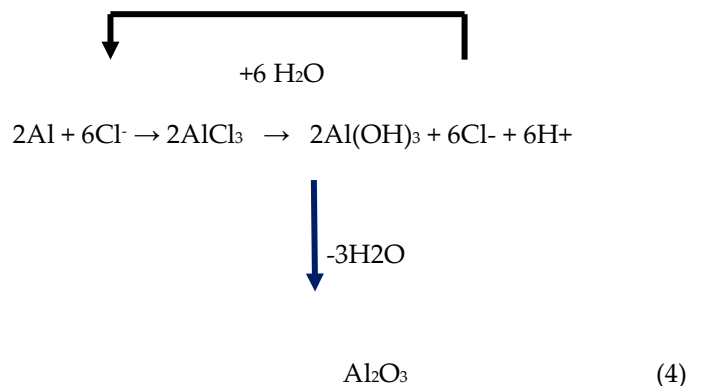
In the production process of wafer fab and via holes, Al of M1 reacts with Cl to generate aluminium trichloride ($AlCl_3$). Because aluminium trichloride is water soluble. Therefore, when it encounters water vapor, a further chemical reaction can produce HCl, which is later decomposed into Cl ions again. The Cl ions could further react with Al to form aluminium trichloride. This repeated chemical reaction process is so-called "Cl-chain chemical

reaction". As a result of the "Cl-chain chemical reaction", only a small amount of Cl ions could propagate in chemical reactions repeatedly, and finally it causes very intensive Cl corrosion reactions even with a small amount of Cl ions.

On the other hand, during chemical reactions, one of the by-products from the chemical reaction is aluminium hydroxide. In the production process, aluminium hydroxide would be dehydrated to form alumina. These aluminium oxides and part of aluminium trichloride will generate aluminium oxychloride ($Al_xCl_yO_z$) through a series of physical and chemical reactions.

With the progress of the chemical reactions, the mixtures of alumina and aluminium oxychloride would continuously grow up, just like worms slowly formed and crawled out of via holes, forming the worm-like defects as observed. Finally, the reaction in between Alumina and Al chloride produced aluminium oxychloride ($Al_xCl_yO_z$). They could grow up from the bottom of the Vias, and eventually form the worm-like defects in and outside the Via holes.

3.2. Failure Analysis

In via process of wafer fabrication, the worm-like defects could occupy the entire via holes or part of the via holes. In the subsequent via metal filling, some vias would show partial via filling, resulting in empty via or via hole issues, which in turn directly the BOEL process integrity.

For the failure via structures, we performed the failure analysis by deprocessing (delayering), and then top-down and cross-sectional SEM analysis. Figure 6 showed the top-down SEM images after deprocessing. As shown by Figure 6, the good Vias essentially showed good metal filling (up of the Figure 6), but in the bad area, one Via showed apparent partial filling due to the worm-like defect (down of Figure 6).

We also performed cross-section FIB (focused ion beam)-SEM analysis. The cross-sectional SEM analysis results were shown in Figure 7. It is clear that the via in the affected lots showed partial filling with a big void at the via bottom (down of the Figure 7) and the FIB-SEM result showed that in the good sample without the worm-like defect, the Via was completed to fill in (up of the Figure 7).

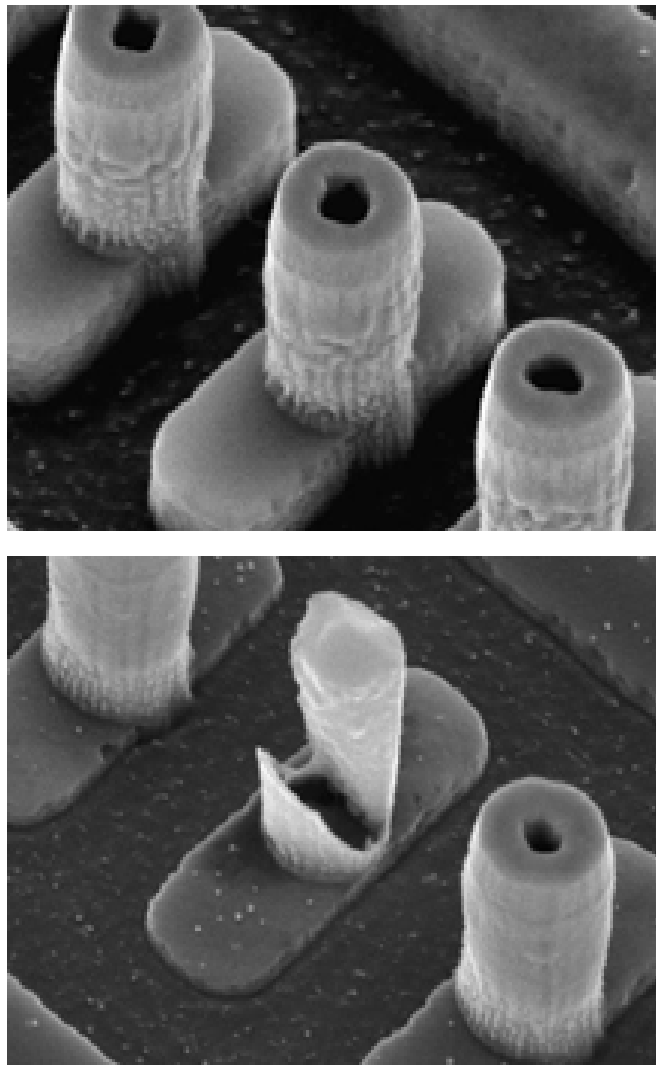Figure 6: The delayering results showed in good area, the Vias had good metal filling (up), but in bad area, partial via filling was observed due to the worm-like defect (down).
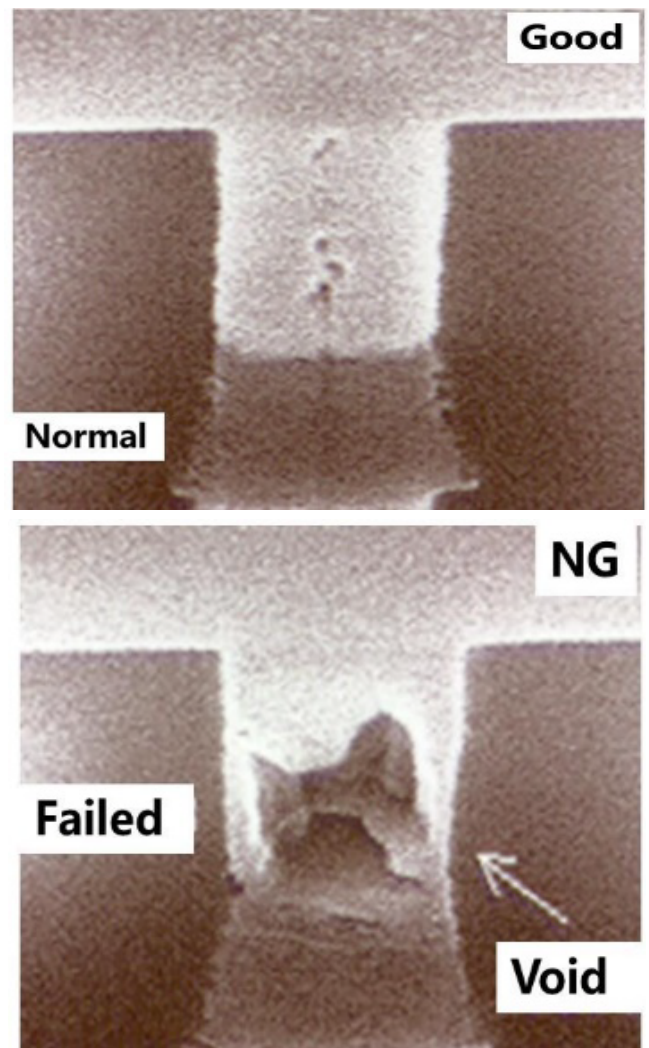

Figure 7: FIB crass sectional result showed that in the good sample without the worm-like defect, the Via was completed to fill in (up). But non good (NG) sample with the worm-like defect, the Via was not completed to fill in and with the void (down).

3.3. C. Root Cause Identification and Solution

Inline investigations and analysis reveal interesting characteristics of the worm-like defects. KLA scan maps of the affected wafers showed a distinct bracket signature (refer to Figure 8). There was also no single wafer orientation or alignment with respect to the notch. Another characteristic was that the first slot was typically the most severely affected wafer compared to the rest of the wafers in the lot. It has also been observed that the occurrence of the worm-like defects was intermittent with no common tool, device/part, or layer. It also occurred even with environmental Cl levels safely below the specification limit.
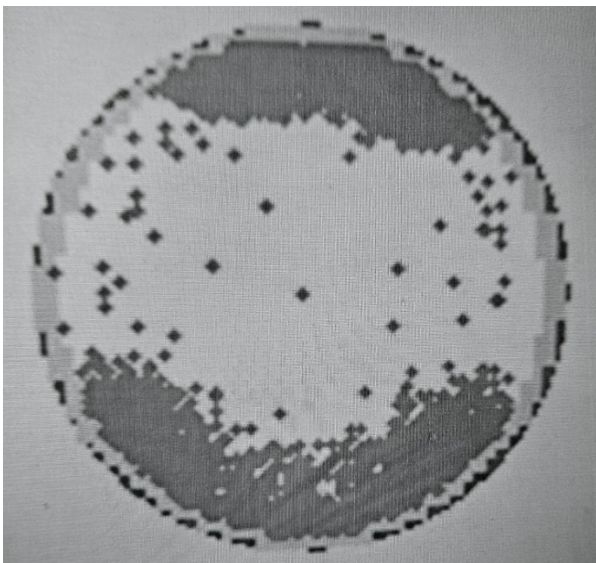

Figure 8: KLA scan map of the wafer affected with the worm-like defects showing bracket signature.

Based on the abovementioned characteristics of the defect, residual chlorine is believed to have originated from the mini-environments (SMIF pod) used to transport the wafers during IC fabrication. After etch, the photoresist is removed by plasma resist strip (PRS) process. In the PRS tool, there is a possibility of pod switching. For instance, a SMIF pod may contain wafers that have undergone polysilicon etch which uses Cl-based etchant gases (refer to Table 1). As a result, the SMIF pod traps residual Cl. After the PRS step, it is possible for wafers with exposed Al metal to be contained in a Cl-contaminated SMIF pod that was previously used during polysilicon etch, a Cl-based etch process. The residual Cl inside the contaminated pod attacks the exposed Al metal in the presence of ambient moisture and forms corrosion products as discussed in the earlier section.

The pod-switching scenario described above occurs at random. This explains why only a few and very intermittent cases occur, and that no common tool, device/part or layer has been derived. Furthermore,

worm-like defects are only seen after via etch and not after metal etch. This is because metal etchers employ *in situ* resist strip where pod switching is not possible.

The distinct bracket signature in KLA scan maps matches the exposed sections of the wafers when placed inside the cassette (see Figure 4). In other words, only those sections exposed to the SMIF pod are affected with worm-like defects.

As the topmost wafer is the most exposed wafer, it is also the most severely affected, hence producing the "first wafer" effect. These observations reinforce the theory that corrosion is due to SMIF pod contamination. A feasible solution therefore is to eliminate the possibility of pod switching between a pod used for Cl-based etch process and a pod with exposed Al metal.

4. Conclusions

In this work, we performed failure analysis and mechanism studies of the Worm-like defects in Via holes of wafer fab. The Worm-like defects occurred after Via holes etching processes, which was caused by Cl contamination and corrosion. We proposed Cl-chain chemical reaction mechanism related to Cl-induced chemical corrosion processes: a). Cl-corrosion is self-sustained; b). A small amount of Cl is sufficient to trigger corrosion; and c). Cl and Al form Al chloride ($AlCl_3$). Because $AlCl_3$ is water-soluble, it can release Cl ions again when it encounters water vapor, then further corroding Al metal. Therefore, a small amount of Cl ions could be repeatedly used in chemical reactions, causing a Cl-chain chemical reaction, which produces alumina, a corrosion product. These aluminum oxides and part of aluminum trichloride would generate aluminum oxychloride ($Al_xCl_yO_z$) through a series of physical and chemical reactions. These by-products induced by Cl-chain reaction processes accumulated and grew from the bottom of the Vias, and eventually formed the Worm-like defects in and outside the Via holes. In the subsequent via metal filling, some vias would appear that the metal filling would not enter that cause voids in Vias and finally after M2 went up, it would cause M1 and M2 to open or leak directly.

Conflict of Interest

The authors declare no conflict of interest.

References

[1]. C. J. Mogab, "Dry Etching," in *VLSI Technology*, S. M. Sze, Ed., McGraw-Hill, 1983, pp. 307.

[2]. H. Younan et al., "A Study on Non-Stick Aluminum Bondpads due

to Fluorine Contamination using SEM, EDX, TEM, IC, Auger, XPS & TOF-SIMS Techniques," in *Proc. 28th Int. Symp. Testing & Failure Analysis (ISTFA'2002)*, Phoenix, AZ, USA, Nov. 3-7, 2002, pp. 495-504.

[3]. H. Younan et al., "A Study on Fluorine-Induced Corrosion on Microchip Aluminium Bondpads," in *Proc. 29th Int. Symp. Testing & Failure Analysis (ISTFA'2003)*, Santa Clara, CA, USA, Nov. 2-6, 2003, pp. 249-255.

[4]. H. Younan et al., "Studies of Fluorine-induced Corrosion Defects on Microchip Al Bondpads and Elimination Solutions," in *Proc. 34th Int. Symp. Testing and Failure Analysis (ISTFA 2008)*, Portland, OR, USA, Nov. 2-6, 2008, pp. 285-290.

[5]. H. Younan, "Studies and Application of Auger Monitoring System for Quality Control and Assurance of Al Bondpads," in *Proc. 42nd Int. Symp. Testing and Failure Analysis (ISTFA 2016)*, Fort Worth, TX, USA, Nov. 6-10, 2016.

Isolation and Characterization of the Bioplastic Producing Bacteria Using Low-Cost Substrate, Sawdust

Anam Javaid[1], Sumaira Aslam[1,*], Hira Qaisar[1], Farhat Batool[1], Rimsha Javed[1], Muhammad Waqas Qaisar[2]

[1] Department of Zoology, GC Women University, Faisalabad, 38000, Pakistan

[2] Department of Mechanical, Mechatronics and Manufacturing Engineering, University of Engineering and Technology, Lahore (Faisalabad Campus), 38801, Pakistan

*Corresponding author: Sumaira Aslam, 092-333-4932868, dr.sumairaaslam@gcwuf.edu.pk

ABSTRACT: Plastics are routinely used in the packaging of materials as well as in industrial production. However, once in the environment, they are non-biodegradable, posing severe threats to the ecosystems. Bioplastic replaces conventional plastic, which is biodegradable due to its biological origin and does not affect environment. Sawdust is a very important agro-waste screened as a substrate for bioplastic production. In the present study, bacteria capable of producing bioplastic by utilizing sawdust as a cheap substrate were isolated and optimized for bioplastic production. Eight sawdust utilizing bacteria were isolated and the strains were designated as SD1 to SD8. These indigenous bacterial isolates were screened for bioplastic production using Sudan Black B Staining. Among the bacterial isolates, the bioplastics (PHB) production levels were 0.046 g/mL to 0.32 g/mL, while the maximum PHB (g/ml) production (0.32 ± 0.008g/mL) was given by SD2 isolate identified as the *Bacillus cereus*-SD2 strain through 16SrDNA sequencing. The isolate SD2 was optimized for bioplastic production at different growth conditions. The best temperature for the bioplastic production was 37°C in the saw dust containing low-cost medium and yielded 0.32 ± 0.00 optical density at wavelength 235 nm of crotonic acid. The isolate SD2 showed a higher PHB (g/ml) yield of 0.31 ± 0.008 under alkaline conditions of pH 9. Sufficient oxygen was required for the higher PHB (g/ml) production by the bacterial isolate SD2, which yielded a 0.32 ± 0.006 level of PHB as compared to the non-aeration. The *Bacillus cereus*-SD2 is a promising bacterial which can produce environmentally friendly bioplastics using low-cost substrate. Finding more growth condition for enhanced bioplastics yields in future are suggested to scale up the production process at industrial level.

KEYWORDS: Bioplastics, PHB production, Agri wastes-based bioplastics

1. Introduction

Plastic, a type of polymer, has influenced every part of the modern world mainly because of its lightweight, low cost, robustness and flexibility [1]. In recent COVID -19 pandemic the use of plastic increased in medical fields and disposable packaging [2]. They are mostly made from carbon atoms derived from fossil fuels [3]. A range of additives or plasticizers are also used in their production. Along with the scores of benefits associated with plastics, the plastic debris and plasticizers discharged from them have become an environmental hazard today [4]. Most of the plastics, particularly the petroleum-based are highly resistant to biodegradation, resulting in negative impacts on the physical and biological aspects of the environment [5]. One of the sustainable and futuristic solutions of this issue is the development of bioplastics.

Bioplastics are the materials synthesized by deriving all carbon from renewable feedstock. Owing to their biodegradable nature, they can substitute for conventional plastics. They are made up of monomeric chains that are linked by ester bonds, also known as polyesters. Among many types and different degrees of biodegradability,

polyhydroxyalkonate (PHA) and polyhydroxybutyrate (PHB) are very common bioplastics. They are produced by a variety of bacteria as energy reserves under deficient conditions [6]. Polyhydroxybutyrate (PHB) potential candidate can also be obtained by microbial fermentation and is intensively researched [7-8]. The PHB market is predicted to reach $98 million by 2024 with a compound annual growth rate of 11.24% [9].

However, as eco-friendly alternatives to synthetic plastics, the major limiting factor in the wider adaptability of bioplastics is the expensive carbon substrate used in the fermentation process [10]. As a biodegradable polymer with characteristics resembling those of conventional plastics, polyhydroxyalkanoate (PHA) is seen as a potential replacement for plastics made from petrochemical derivatives. Hundreds of bacteria can reportedly store PHA in prokaryotic cells to sustain their own development and metabolism [11]. Paddy straw is one of the agricultural wastes produced in large quantities during the rice harvest [12] Wide variety of cost-efficient substrates, such as wheat bran, rice bran, ragi bran, jambul seed powder and orange were screened for PHA production. In numerous studies sawdust was also employed to produce PHA [13-14]. It could be potentially inexpensive and renewable feedstock for production of PHA as the woodworking industry generates this solid waste.

The primary factor restricting the large-scale manufacture of PHAs at the moment is the higher production cost. According to various polymer types, the cost of producing PHAs has increased to 4,000–15,000 US$/Mt, which is roughly 4–10 times more expensive than petrochemical-based polymers [15]. Thus, recent studies have aimed to utilize low-cost feedstocks such as agricultural, food processing, and municipal wastes [16]. Therefore, in present study, we demonstrated the production of PHB from saw dust isolates as low-cost feedstock.

2. Methodology

2.1. Sampling

The bioplastic-producing bacteria were isolated from the soil samples collected from industrial area of the city Kasur (31.12° North latitude and 74.45° East longitude), Pakistan and placed in a sterile glass bottle under standard sterilization conditions. The samples were brought to the Microbiology and Biotechnology Laboratory of Zoology Department, GC Women University, Faisalabad and were stored in the fridge at 4°C for later use.

2.2. Enrichment of sawdust substrate utilizing bacteria

The substrate media was prepared by adding 2 g of sawdust in flask, containing 50 mL of distilled water. This flask containing substrates was then autoclaved at 121°C and 15 lbs. pressure for 15 minutes. After autoclaving, when flasks containing the substrates reached room temperature, 1 g of soil sample was added to each of the flasks. They were then incubated for 48 h at room temperature.

2.3. Isolation and characterization of the bacteria

A specific volume of the enrichment culture was spread with a sterilized glass spreader over the nutrient agar plate. The agar plates were incubated at 37°C for 24 h and growth of the bacterial isolates was observed and recorded. The bacterial colonies were processed for pure culturing and morphological and physicochemical characteristics of the bacterial isolates were determined [17].

2.4. Identification of the bacteria by 16SrRNA

The select bacterial isolate was characterized through 16S rDNA sequencing. To achieve this, DNA was extracted from a bacterial culture that had been grown overnight in nutrient broth at 37°C, following the method outlined by Li et al. [18]. For the PCR amplification of the 16S rDNA, the following primers were utilized: 27f (5'-AGATTTGATCMTGGCTCAG-3') and 1492r (5'-GGTTACCTTGTTACGACTT-3'). The PCR reaction mixture comprised the DNA extract, $MgCl_2$, dNTPs, forward and reverse primers, DNA Taq polymerase, and Taq buffer. The PCR process involved an initial denaturation step at 94°C for 3 minutes, followed by 35 cycles of denaturation at 95°C for 30 seconds, an annealing step at 60°C for 2 minutes, and an extension step at 72°C for 1 minute. A final extension step was carried out at 72°C for 30 minutes using a thermal cycler (Hamburg 22331, Germany). The resulting PCR product consisted of amplified bands measuring 1.5 kb, which were subsequently subjected to electrophoresis and visualized under UV light [Gel Doc, Bio-Rad Laboratories, USA]. To purify the DNA bands, a Gene Purification Kit (Fermentas) was employed, following the manufacturer's instructions. Subsequently, sequencing was performed using Big Dye Terminator v3.1 cycle sequencing ready reactions (Macrogen, Korea) at the DNA Sequencing Facility in Korea. The 16S rRNA gene homology search was conducted using BLAST (http://www.ncbi.nlm.nih.gov/BLAST/). The 16S rDNA sequence obtained for the SD2 isolate in this study was submitted to GenBank to obtain an accession number.

2.5. Selection of the Polyhydroxy butyrate (PHB) producing bacteria

The bacterial isolates from the agar slants were revived in nutrient broth. Then these isolates were screened for PHB production following the Sudan Black B staining method [6]. Sudan Black B stain (0.3%) was prepared in 70% ethanol. Then a bacterial smear was prepared. For this purpose, one loop full of bacterial colonies was picked with the help of a sterilized loop and placed in a small drop of sterilized distilled water on a clean glass slide. The smear was prepared with the help of a clean toothpick. Later, the smear was heat fixed. Few drops of Sudan Black B stain solution were poured over the smear and incubated for 10 minutes. Then the slide was washed with distilled water and counter-stained with safranin and left for 5 minutes. The prepared slide was observed under a microscope and the results were noted. All bacteria with PHB production ability were then chosen for further research.

2.6. Preparation of Fermentation Media

The N-limited medium [19] consisting of $(NH_4)_2SO_4$ – 2 g/L; KH_2PO_4 -2 g/L; $MgSO_4.7H_2O$-0.2 g/L; Na_2HPO_4- 0.6 g/L; Yeast Extract - 0.2 g/L and trace elements – 1ml was prepared in distilled water. The composition of the trace element solution was $FeSO_4.7H_2O$ - 10g/L; $ZnSO_4.7H_2O$ - 2.25 g/L; $CuSO_4.5H_2O$ - 1 g/L; $MnSO_4.5H_2O$ - 0.5 g/L; $CaCl_2.2H_2O$ - 0.2 g/L; $Na_2B_4O_7.7H_2O$ - 0.23 g/L; $(NH_4)_8Mo_7O_{24}$ - 0.1 g/L and 35% HCl 10 mL/L. The N-limited medium was supplemented with 1% of substrates, i.e., sawdust, as carbon source.

2.7. Quantitative determination of the PHB

Fermentation media with the substrate (Tables 3) was inoculated with the select bacteria. After 48 hours of incubation, 10 mL of bacterial culture was centrifuged at 6000 rpm for 15 min. Then, the pellet was suspended in 5 mL of sterile water and dried for 24 h at 100ºC. To the cell suspension, 5 mL of sodium hypochlorite solution was added and incubated at 60ºC for 1 h [20]. This suspension was centrifuged at 6000 rpm for 15 min and the supernatant was separated. To extract cell lipids and other molecules (except PHB) from the supernatant, we added 5 mL of 96% (1:1 v/v) ethanol and acetone. Now, 10 mL of chloroform were added to the tube by placing it in a hot water bath (60℃). Chloroform was evaporated to obtain PHB crystals. 10 mL of 98% H_2SO_4 was added at 60℃ and kept for 1 h to convert PHB crystals into crotonoic acid. After cooling to 25°C, the amount of PHB was determined spectrophotometrically at 235 nm against H_2SO_4 as a blank with crotonoic acid as a standard [21].

2.8. Optimization of the PHB production

The select bacterial isolate was optimized for different physical conditions to obtain higher PHB crystal yields. The effects of pH (5, 7, 9), temperature (25°C, 37°C, 50°C) and aeration conditions (aeration, non-aeration) on PHB production were recorded. All experiments were conducted in replicates of three. The statistical analysis was performed to find the significant difference among different conditions.

3. Results and Discussion

Bioplastics are biodegradable plastics, produced cheaply by using agro-industrial wastes and as a result are considered non-harmful for our environment. These agro-industrial wastes are converted into simple sugars by bacterial enzymes and used for their energy yields [22].

3.1. Isolation of PHB producing bacteria from industrial soil

In the present project, eight sawdust utilizing bacteria designated as SD1, SD2, SD3, SD4, SD5, SD6, SD7 and SD8 were isolated from sawdust containing medium. Their colonial and physicochemical characterization are presented in the Table 1 and 2.

Table 1: Colonial characterization of the saw dust utilizing bacterial isolates on the Nutrient Agar plates

Isolate Code	Shape	Margin	Elevation	Size	Texture	Appearance	Pigmentation	Optic property
SD1	Circular	Entire	Raised	Small	Rough	Dull	White	Opaque
SD2	Circular	Entire	Slightly raised	Small	Smooth	Shiny	Off-White	Opaque
SD3	Circular	Entire	Raised	Small	Rough	Dull	White	Opaque
SD4	Irregular	Undulate	Slightly raised	Small	Smooth	Shiny	Off-White	Opaque

SD5	Irregular	Undulate	Flat	Small	Rough	Dull	Off-White	Translucent
SD6	Irregular	Undulate	Flat	Small	Rough	Dull	Off-White	Translucent
SD7	Irregular	Undulate	Slightly raised	Small	Smooth	Shiny	Off-White	Opaque
SD8	Circular	Entire	Raised	Small	Rough	Dull	White	Opaque

Table 2: Physicochemical properties of saw dust utilizing bacterial isolates

Isolate Code	Shape of the cell	Endospore Staining	Gram Staining	Motility Test	Catalase Test	Oxidase Test	Genus Identified
SD1	Rod Shape	Terminal Endospore	Gram Positive	Motile rods	Positive	Negative	Bacillus
SD2	Rod shape	Endospore	Gram Positive	Motile rods	Positive	Negative	Bacillus
SD3	Diplobacilli	Absent	Gram Negative	Non-motile	Positive	Negative	Klebsiella
SD4	Rod Shaped	Terminal Endospore	Gram Positive	Motile rods	Positive	Negative	Bacillus
SD5	Diplobacilli	Central Endospore	Gram Positive	Motile rods	Positive	Negative	Bacillus
SD6	Diplobacilli	Central Endospore	Gram Positive	Motile rods	Positive	Negative	Bacillus
SD7	Rod Shaped	Terminal Endospore	Gram Positive	Motile rods	Positive	Negative	Bacillus
SD8	Diplobacilli	Absent	Gram Negative	Non-motile	Positive	Negative	Klebsiella

3.2. Qualitative Screening of bacterial isolates for bioplastic production

All of the bacterial isolates from the sawdust substrate were initially screened qualitatively by the Sudan Black B staining method, for PHB production. PHB granules were present in the bacterial cells in the form of dark granules. The photomicrographs of isolates showing the PHB granules produced in the form of dark spots in the bacterial cells are given in Fig. 1. Sawdust, being a waste, is affordable and easily available substrate. It contains cellulose, hemicellulose and lignin. Owing to these nutrients, it was used in this study as a substrate to optimize the PHB production. Sawdust is one of the substrates with a higher C/N ratio. The higher carbon and lower nitrogen levels are the major requirements for the higher PHB yields. The nitrogen-limiting condition promotes higher levels of PHB [23], whereas higher nitrogen levels inhibit PHB production by bacteria [24].

Five sawdust utilizing bacterial isolates, SD1, SD2, SD3, SD4 and SD5 showed higher bioplastic granules accumulation. Those showing granules were further assessed for the quantitative production of PHB.
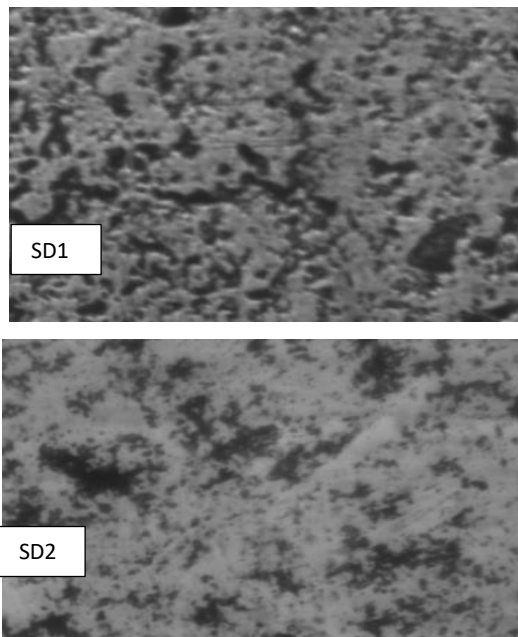
Figure 1: Photomicrographs of isolates SD1 and SD2 showing the PHB accumulates as dark granules in the bacterial cells.
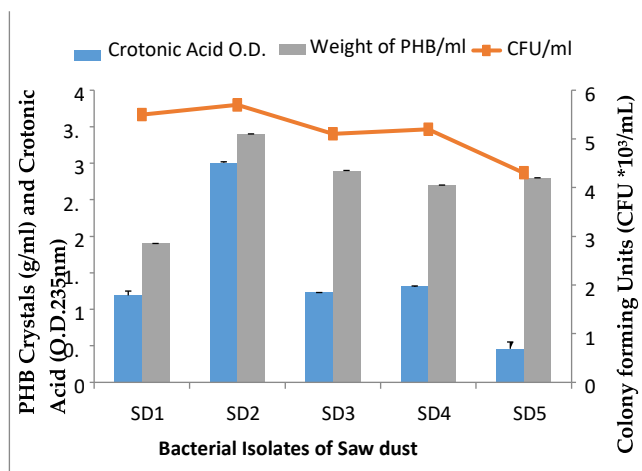

Figure 2: The PHB accumulation and crotonic acid production (O.D. 235nm) by the select bacterial isolates using sawdust as a low-cost substrate after 48 hours of incubation at 37°C

3.3. Screening of the bacterial isolates utilizing sawdust as a low-cost waste for PHB production

Five distinct bacterial colonies isolated from the industrial soil on the agar plates containing saw dust showed varying levels of CFU/mL, PHB crystal and crotonic acid (Fig. 2-4). Highest CFU/mL was obtained by SD2 (5.7×10^3) which was higher than the SD1 (5.5×10^3), SD3 (5.1×10^3), SD4 (5.2×10^3) and SD5 (4.3×10^3). Maximum PHB (g/mL) crystals production was obtained by SD2 (0.30g ± 0.001/ml) as compared to SD1 (0.19g ± 0.001/ml), SD3 (0.29 g ± 0.001/ml), SD4 (0.27 g ± 0.001/ml) and SD5 (0.28g ± 0.001/ml). SD2 PHB crystals produced higher crotonic acid of 0.31 ± 0.00 optical density at wavelength 235 nm as compared to

the SD1 (0.11 ± 0.09), SD3 (0.12 ± 0.15), SD4 (0.13 ± 0.009) and SD5 (0.04 ± 0.09).

Figure 3: PHB crystals obtained by the bacterial isolates using sawdust as a low-cost substrate
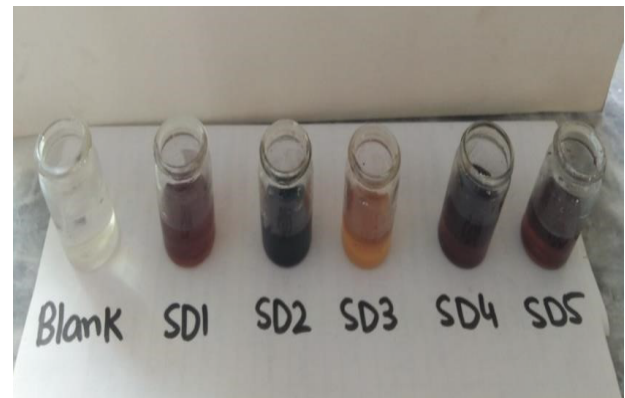

Figure 4: Crotonic acid (O.D. 235nm) obtained by selected bacterial isolates using bread crumbs and sawdust as low-cost substrates

3.4. Optimization of the PHB yields by the bacterial isolate SD2

The select bacterial isolates (SD2) with higher PHB crystal accumulation (upto 0.33 g/mL) were optimized for PHB production under varying physical conditions at 48 h of incubation. The effect of pH (5, 7, 9,), temperature (25°C, 37 °C, 50 °C) and aeration conditions (aeration, non-aeration) on PHB production by the SD2 isolate was assessed and is presented in Figure 5, 6 and 7. The crystals so produced were further assessed quantitatively by sulphuric acid assay. The pH 9 was found to be optimal for higher PHB and crotonic acid production by the isolate SD2. Many researchers [18] have reported that neutral pH is optimal for maximum PHB production. Oxygenated conditions favor more PHB and crotonic acid production, while the non-aeration conditions lessen the production of PHB. Bacillus species are mostly aerobes that need oxygen to survive. More oxygen concentration favors more bacterial growth and in turn, more PHB is accumulated [25]. It is reported that bacterial cell density and PHB are directly proportional to each other up to a certain level [26].
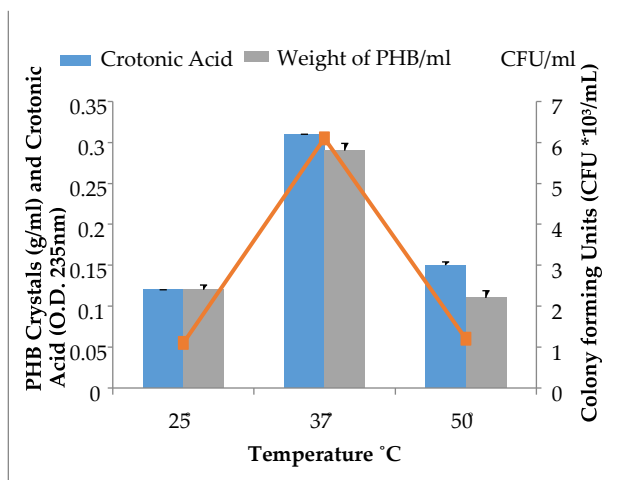
Figure 5: Effect of different temperature (℃) on PHB production by SD2 after 48 hours of incubation at pre-optimal conditions
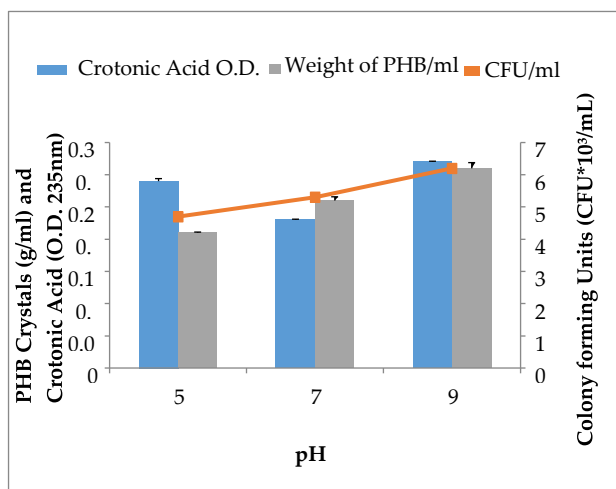

Figure 6: Effect of different pH (5, 7, 9) on PHB production by SD2 after 48 hours of incubation at pre-optimal conditions

Maximum bacterial growth and PHB production of SD2 ($6.3×10^3$ CFU/mL; 0.32 g/mL) was obtained at 37℃ after 48 h of incubation. Bacterial isolates with high growth rate and ideal procedure conditions have been reported for 90% of PHB production [27]. High temperature does not favor increased PHB production as it disrupts the cytoplasmic membrane of the cell. The PHB cannot be stored in the bacterial cell in the presence of high temperature [28]. As temperature reaches its extreme, a sharp decline in the PHB production occurs. Bacterial growth and PHB production are related to each other. When bacterial growth increases, polyhydroxybutyrate also increase to maximum level. After a certain level, PHB production starts decreasing because nutrient depletion occurs and bacteria starts using PHB to obtain the energy [29].
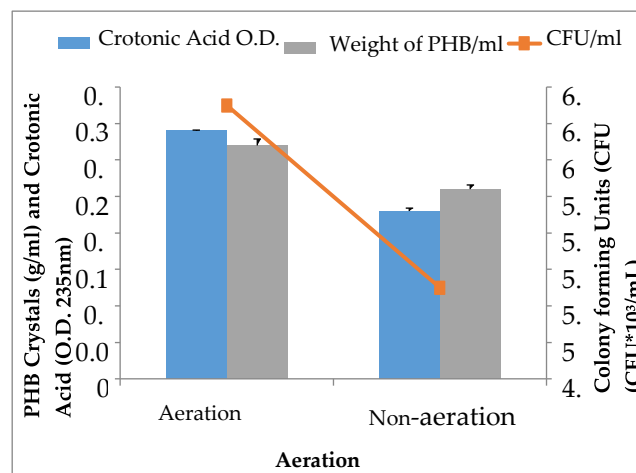

Figure 7: Effects of oxygen conditions on the PHB production by SD2 after 48 h of incubation at pre-optimal temperature and pH

3.5. Identification of the PHB producing SD2 isolate by 16Sr DNA sequencing

The PHB producing SD2 isolate was identified as *Bacillus cereus*-SD2 through BLAST analyses and was allotted OR607937 accession number on submission to NCBI database. Most of the sawdust utilizing bacterial isolates belonged to the Bacillus genus. Many reporters have described *Bacillus* species ideal for PHB production [30].

4. Conclusion

In conclusion, our study successfully explored the utilization of sawdust, a significant agricultural waste product, as a substrate for the production of bioplastics. Through a systematic approach, we isolated and optimized bacteria with the ability to produce bioplastics using sawdust as an economical and sustainable substrate. Among the eight indigenous bacterial isolates obtained from an industrial soil sample, *Bacillus cereus* strain SD2 stood out as the most proficient producer of polyhydroxybutyrate (PHB) when exposed to sawdust. These findings underscore the substantial potential of sawdust as a valuable resource for bioplastic production, thereby addressing the environmental concerns associated with traditional plastics. Moreover, the exceptional performance of *Bacillus cereus* strain SD2 in bioplastic production, when subjected to optimized conditions, represents a promising avenue for developing eco-friendly alternatives to conventional plastics. For future prospects, further research can focus on scaling up the production process, exploring different strains, and refining the conditions to enhance bioplastic yields. Additionally, investigating the biodegradability and overall environmental impact of these bioplastics will be crucial to

fully assess their sustainability and applicability in reducing plastic pollution. Ultimately, our study contributes to the ongoing efforts to transition toward more sustainable and environmentally responsible materials in various industries.

References

[1]. S. Carmen, "Microbial capability for the degradation of chemical additives present in petroleum-based plastic products: A review on current status and perspectives," Journal of Hazardous Materials, vol. 402, pp. 123534,2021,doi.org/10.1016/j.jhazmat.2020.123534.

[2]. S.K. Bhatia, S.V. Otari, J.M. Jeon, R. Gurav, Y.K. Choi, R.K. Bhatia, A. Pugazhendhi, V. Kumar, J. RajeshBanu, J.J. Yoon, K.Y. Choi and Y.H. Yang, "Biowaste-to-bioplastic (polyhydroxyalkanoates): Conversion technologies, strategies, challenges, and perspective," Bioresour. Technol., vol. 326, pp. 124733, 2021,

[3]. I. E. Napper and R.C. Thompson, "Plastic Debris in the Marine Environment: History and Future Challenges," Global Challenges, vol. 4, no. 3, pp. 1900081, 2020, doi.org/10.1002/gch2.201900081.

[4]. M. A. Burgos-Aceves, H. G. Abo-Al-Ela and C. Faggio, "Physiological and metabolic approach of plastic additive effects: Immune cells responses," Journal of Hazardous Materials, vol. 404, pp. 124114,2021,doi.org/10.1016/j.jhazmat.2020.124114.

[5]. T. Narancic and K.E. O'Connor, "Plastic waste as a global challenge: are biodegradable plastics the answer to the plastic waste problem?" Microbiology, vol. 165, no. 2, pp. 129–137, 2019, doi.org/10.1099/mic.0.000749 .

[6]. S. A. Kojuri, K. Issazadeh, Z. Heshmatipour, M. Mirpour and S. Zarrabi, "Production of Bioplastic (Polyhydroxybutyrate) with local Bacillus megaterium isolated from petrochemical wastewater," Iranian Journal of Biotechnology, vol. 19, no. 3, pp. 2849, 2021,doi.org/10.30498/ijb.2021.244756.2849.

[7]. J. Fradinho, L. D. Allegue, M. Ventura, J. A. Melero, M. A. M. Reis and D. Puyol, "Up-scale challenges on biopolymer production from waste streams by purple phototrophic bacteria mixed cultures: A critical review," Bioresour. Technol. Vol. 327, pp. 124820, 2021,

[8]. J.d.J. Franco-Le´on, E. Arriola-Guevara, L. A. Su´arez-Hern´andez, G. Toriz, G. Guatemala- Morales and R. I. Corona-Gonz´alez, "Influence of supplemented nutrients in tequila vinasses for hydrogen and polyhydroxybutyrate production by photofermentation with Rhodopseudomonas pseudopalustris." Bioresour. Technol. Vol. 329, pp.124865, 2021,

[9]. R. Sirohi, J. Prakash Pandey, V. Kumar Gaur, E. Gnansounou and R. Sindhu, "Critical overview of biomass feedstocks as sustainable substrates for the production of polyhydroxybutyrate (PHB)," Bioresour. Technol, vol. 311, pp. 123536, 2020,

[10]. R. Z. Sayyed, S. S. Shaikh, S. J. Wani, M. T. Rehman, M. F. Al Ajmi, S. Haque and H. A. El Enshasy, "Production of Biodegradable Polymer from Agro-Wastes in Alcaligenes sp. and Pseudomonas sp.," Molecules, vol. 26, no. 9, pp. 2443, 2021, doi.org/10.3390/molecules26092443.

[11]. L. Kaur, R. Khajuria, L. Parihar, and G. Dimpal Singh, "Polyhydroxyalkanoates: Biosynthesis to commercial production- A Review," Journal of Microbiology, Biotechnology and Food Sciences, vol. 6, no. 4, pp. 1098–1106, 2017,doi.org/10.15414/jmbfs.2017.6.4.1098-1106.

[12]. J. Wang, S. Liu, J. Huang, and Z. Qu, "A review on polyhydroxyalkanoate production from agricultural waste Biomass: Development, Advances, circular Approach, and challenges," Bioresource Technology, vol. 342, pp. 126008,2021,doi.org/10.1016/j.biortech.2021.126008.

[13]. T. M. Keenan, S. W. Tanenbaum, A. J. Stipanovic and J. P. Nakas, "Production and Characterization of Poly-β-hydroxyalkanoate Copolymers from Burkholderia cepacia Utilizing Xylose and Levulinic Acid," Biotechnol. Prog. Vol. 20, pp. 1697–1704, 2004,

[14]. J. A. Silva, L. M. Tobella, J. Becerra, F. Godoy and M. A. Martínez, "Biosynthesis of poly-β-hydroxyalkanoate by Brevundimonas vesicularis LMG P-23615 and Sphingopyxis macrogoltabida LMG 17324 using acid-hydrolyzed sawdust as carbon source." J. Biosci. Bioeng. Vol. 103, pp. 542–546, 2007,

[15]. J. A. Posada, J. M. Naranjo, J. A. López, J. C. Higuita and C. A. Cardona, "Design and analysis of poly-3-hydroxybutyrate production processes from crude glycerol," Process Biochemistry, vol. 46, no. 1, pp. 310–317, 2011,doi.org/10.1016/j.procbio.2010.09.003.

[16]. R. Sindhu, A. Manju, P. Mohan, R. O. Rajesh, A. Madhavan, K. B. Arun, S. H. Hazeena, A. Mohandas, S. P. Rajamani, A. Puthiyamadam, P. Binod and R. Reshmy, "Valorization of food and kitchen waste: An integrated strategy adopted for the production of poly-3-hydroxybutyrate, bioethanol, pectinase and 2, 3-butanediol," Bioresour. Technol, vol. 310, pp. 123515, 2020,

[17]. H. J. Benson 2020. 'Microbiological Applications, Laboratory Manual in General Microbiology'' W.M.C. Brown Publishers, Dobuque, USA

[18]. H, Li, F. Medina, S. B. Vinson, C.J. Coates"Isolation , characterization and molecular identification of bacteria from red imported ant midgut'' journal of invertebrate pathology, vol. **89**, pp. 203-209, 2005.

[19]. R. Sindhu, B. Ammu, P. Binod, S. K. Deepthi, K. B. Ramachandran, C. R. Soccol and A.Pandey, "Production and characterization of poly-3-hydroxybutyrate from crude glycerol by Bacillus sphaericus NII 0838 and improving its thermal properties by blending with other polymers," Brazilian Archives of Biology and Technology, pp. 54, no. 4, pp. 783–794, 2011, doi.org/10.1590/S1516-89132011000400019.

[20]. S. V. Kumar and S. Ashish, "Production of Polyhydroxybutyrate from Cafeteria Waste: An Environment Friendly Approach," Pharmacia, vol. 1, no. 2, pp. 47–51. 2011,

[21]. A. Soam, A. K. Singh, R. Singh and S. K. Shahi. "Optimization of culture conditions for bio-polymer producing Bacillus mycoides (WSS2) bacteria from sewage," International journal of current innovation and research, vol. 1, pp. 27-32, 2012,

[22]. A. Di Bartolo, G. Infurna and N. T. Dintcheva, "A Review of Bioplastics and Their Adoption in the Circular Economy," Polymers, vol. 13, no. 8, pp. 1229, 2021, doi.org/10.3390/polym13081229

[23]. Lee, Y. R., Fitriana, H. N., ''Molecular profiling and optimization studies for growth and PHB production conditions in Rhodobacter sphaeroides'' Energies, vol.13, no. (23), (2020), doi.org/10.3390/en13236471

[24]. E. Z. Gomaa, "Production of polyhydroxyalkanoates (PHAs) by Bacillus subtilis and Escherichia coli grown on cane molasses fortified with ethanol," Brazilian Archives of Biology and Technology, vol. 57, no. 1, pp. 145–154. 2014, doi.org/10.1590/S1516891320140000100020.

[25]. L. Djerrab, Z. Chekroud, A. Rouabhia, M. A. Dems, I. Attailia, L. I. R. Garcia, and M. A. Smadi, "Potential use of Bacillus paramycoides for the production of the biopolymer polyhydroxybutyrate from leftover carob fruit agro-waste," AIMS Microbiology, vol. 8, no. 3, pp. 318–337, 2022, doi.org/10.3934/microbiol.2022023

[26]. X. R. Jiang, Z. H. Yao, and G. Q. Chen, "Controlling cell volume for efficient PHB production by Halomonas," Metabolic Engineering, vol. 44, pp. 30–37. 2017. doi.org/10.1016/j.ymben.2017.09.004.

[27]. J. A. Posada, J. M. Naranjo, J. A. López, J. C. Higuita and C. A. Cardona, "Design and analysis of poly-3-hydroxybutyrate production processes from crude glycerol," Process Biochemistry, vol. 46, no. 1, pp. 310–317, 2011, doi.org/10.1016/j.procbio.2010.09.003.

[28]. D. Tripathi, A. Yadav, A. Jha and S. K. Srivastava, "Utilizing of Sugar Refinery Waste (Cane Molasses) for Production of Bio-Plastic under Submerged Fermentation Process," Journal of Polymers and the Environment, vol. 20, no. 2, pp. 446–453, 2012, doi.org/10.1007/s10924-011-0394-1.

[29]. W.N. Chaudhry, N. Jamil, I. Ali, M. H. Ayaz and S. Hasnain, "Screening for polyhydroxyalkanoate (PHA)-producing bacterial strains and comparison of PHA production from various inexpensive carbon sources," Annals of Microbiology, vol. 61, no. 3, pp. 623–629, 2011, doi.org/10.1007/s13213-010-0181-6.

[30]. R. Andler, V. Pino, F. Moya, E. Soto, C. Valdés and C. Andreeßen, "Synthesis of poly3-hydroxybutyrate (PHB) by Bacillus cereus using grape residues as sole carbon source," International Journal of Biobased Plastics, vol. 3, no. 1, pp. 98–111, 2021, doi.org/10.1080/24759651.2021.1882049

ANAM JAVAID received the degree of BS (Hons) in Zoology from Government College Women University Faisalabad. She recently completed her M. Phil in Zoology from Government College Women University Faisalabad, Pakistan. Currently, she serves as a lecturer in Government College.

DR. SUMAIRA ASLAM received her PhD degree from Punjab University Lahore, Pakistan. She is serving as an Assistant professor in the Department of Zoology at Government College Women University Faisalabad. Her current research interests are Bio floc technology in aquaculture systems.

HIRA QAISAR received the degree of BS (Hons) in Zoology from Government College Women University Faisalabad. She completed her M. Phil from Government College University Faisalabad. Currently, she is doing PhD degree in Zoology from Government College Women University Faisalabad. Recently she completed her one research project. Her current research interests are Nanotechnology efficiency in Biofloc based Aquaculture systems.

RIMSHA JAVED received the degree of BS (Hons) in Zoology from Government College Women University Faisalabad. She recently completed her M. Phil in Zoology from Government College Women University Faisalabad. Her current research interests are in Microbiology.

FARHAT BATOOL completed her PhD degree in Zoology. She serves as a lecturer in the Department of Zoology at Government College Women University Faisalabad, Pakistan. Her current research interests are in Aquatic Toxicology.

MUHAMMAD WAQAS QAISAR received a B.Sc. degree in Mechatronics and Control Engineering from the University of Engineering and Technology, Lahore, Pakistan in 2022. Currently, he is working toward a Master's Degree in Control Science and Engineering from Shandong University, Jinan, China. His research interests are Control of Mechatronics Systems, Robotics, Power Electronics, and Automation.

Smart Monitoring System for Housing Societies based on Deep Learning and IoT

Neha Koppikar* , **Nidhi Koppikar**

Department of Data Science MPSTME, SVKMs NMIMS University, Mumbai, India

*Corresponding author: Neha Koppikar & neha.koppikar@gmail.com

ABSTRACT: Since 2020, people have been getting their body temperatures checked at every public location, social distancing has become a norm, and it has become essential to know who has been in contact with whom. Therefore, we needed a system that helped us solve these challenges, especially in housing societies, as most of the general public stayed home more than ever. Therefore, it has become essential to safeguard housing societies. There has been a lot of research in building a security system, but there needs to be more research that targets housing societies as the end users. We have devised a possible solution, including a facial recognition system with body temperature sensing on a Raspberry Pi. The best part of our application is the automated data collection page on a web application, which makes collecting facial images more straightforward and faster. Code for this project can be found at: https://github.com/NehaKoppikar/Monitoring-System-for-Housing-Societies-using-Deep-Learning-and-IoT

KEYWORDS Face Recognition, Raspberry Pi, Edge Vision, Body Temperature, Sensors

1. Introduction

The security of housing societies is paramount to all of us. Currently, security services are provided with the help of watchmen or security guards. However, mistakes on their part, intentional or unintended, do happen, and the people held responsible for such anomalies are either our guardians (security guards/watchmen) or the housing society's co-operation. Technology can assist all the stakeholders in making security arrangements watertight to a greater extent. Anomalies due to misjudgment or carelessness considerably affect the residents of the housing society. There can be thefts and burglaries, and in recent times, this inadvertence can act as a catalyst for the spread of the COVID-19 pandemic into our homes. There should be some way to backtrack if anything goes wrong.

There are a lot of researchers working in this domain and have built a lot of systems to combat the COVID-19 situation. When writing this research paper, 211 papers appeared when searching for "COVID-19" at arxiv.org. There are face-recognition attendance systems [1], systems built on embedded devices for calculating body temperature [2], and so many other research papers have already been published on this topic or related topics that we can come across something new every week if not every day. As part of recognizing someone, bio-metrics has changed the attendance world. There was a time when the only way to acknowledge someone officially was their signature, and a lot has changed since then. Various security systems have been built, but no research has been found targeting housing societies.

We can now automatically store a person in the database without the person being actively involved. All that is required from the person is showing up, and the rest is taken care of. Even though it is possible, there is minimal digital initiatives taken to augment security guards in housing societies. This paper targets this gap.

Along with face recognition, checking a person's body temperature has become extremely important in the pandemic. That is why the three main parts of our solution involve face recognition, body temperature sensing, and regularly sending email notifications to a responsible point of contact.

What makes this paper unique is that even though there are many research papers with biometrics in a security system, there was no research that sends automated email reports to a responsible point of contact in a housing society.

The key contributions of this research are as follows:

- Face-Recognition web application built on streamlit

- Body temperature sensing integrated with face-recognition

- Face-recognition and body temperature sensing data stored automatically in a NoSQL database

- Stored data report periodically sent to a responsible point of contact

- Entire application deployed in Raspberry Pi

2. Literature Survey

To be able to build our solution, we referred a few research papers, which include:

1. MaskedFace-Net – A dataset of correctly/incorrectly masked face images in the context of COVID-19 [3]

   This paper is about a dataset built for face-recognition purposes on masked data. Many face-recognition systems are made in a way where the face-recognition algorithm gets triggered once a face is detected, and many times, the face should be entirely facing the input source (camera). A significant challenge faced by face-recognition systems was met because faces were not detected when covered in a mask. Rebuilding a design as per the requirement needs a vast dataset.

   The dataset on which this research paper is based helps rebuild face-recognition systems on an existing algorithm, FaceNet [4].

   This paper is better because it also addresses the issue of people needing to wear a mask properly. The dataset is labeled so the person is correctly masked or incorrectly masked. If incorrectly masked, it also addresses whether it is due to an uncovered chin, uncovered nose, or uncovered nose and mouth.

2. Monitoring System Heartbeat and Body Temperature Using Raspberry Pi.

   This paper concerns a wireless sensor network (WSN) system to monitor body temperature and heartbeat. The authors of this paper have built this system using Raspberry Pi and Arduino. They have also created a user-friendly website.

   We have taken inspiration from this paper to build the body temperature component of our system.

3. Impact of thermal throttling on long-term visual inference in a cpu-based edge device [5]

   This paper is a comparative study on various levels. It compares multiple Raspberry Pi devices, multiple versions of operating systems, and different CNN-based algorithms, with or without a fan. The results are tested with as many combinations as possible; fans improve efficiency irrespective of the variety they are tested on.

   We tried to use a fan in our approach as well. The issue we found was that we could use the camera or the fan, as the camera came in the way of the fan when it rotated, affecting the camera's connection with the Raspberry Pi board.

4. Smart Security for an Organization based on IoT [6]

   This paper concerns a security system to safeguard an organization from fire and intruders. The researchers have built an android application, which acts as an output source in case any anomaly gets detected.

5. Development of Face Recognition on Raspberry Pi for Security Enhancement of Smart Home System [7]

This paper is about a face-recognition system that is built for houses. It magnetically locks or unlocks the door based on the output of the face-recognition model.

This approach highly inspires our face-recognition system.

3. Research Design

The research methodology was designed as follows:

3.1. Define Research Problem

Our research problem is to build a security system to store when a person enters a housing society and their body temperature. We also wanted to ensure that the data is collected from the application deployed on an embedded device.

3.2. Literature Review

After defining the problem statement, we individually reviewed similar papers on Google Scholar.

3.3. Architecture Design

We designed the architecture for the application, as shown in figure 1.
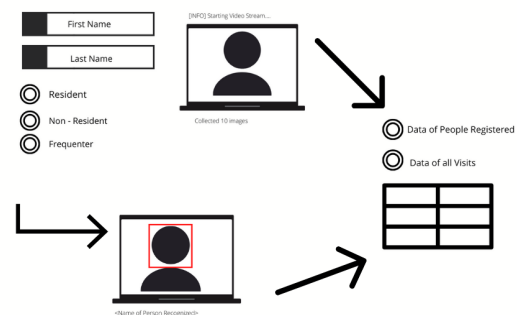

Figure 1: Architecture Design

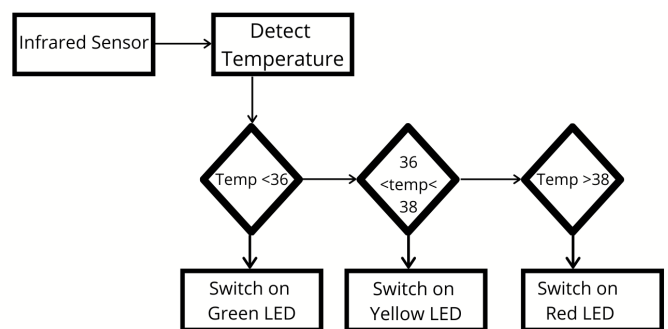For body temperature sensing, we designed the architecture as shown in figure 2.

Figure 2: Body Temperature Architecture Design

3.4. Data Collection

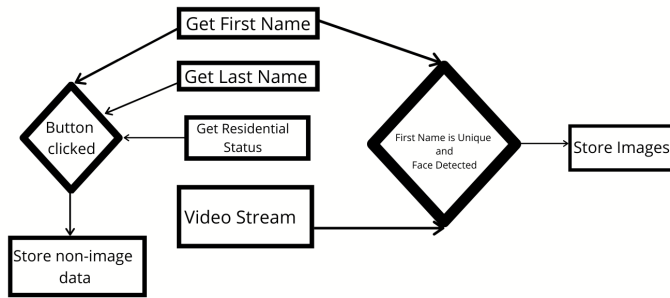Data was collected through the web application [8], as shown in figure 3.

Figure 3: Data Collection

3.5. Building the application

We tried various frameworks and decided to build the application on Python Streamlit as it had fewer challenges and a faster turnaround time.

4. Proposed Work

4.1. Features (and our contributions)

4.1.1. Face-Recognition

We have used Adam Geitgey's Face Recognition library on the Streamlit framework. Using the same library, we also generated face embeddings.

This face-recognition algorithm is a series of several related problems:

- Identify a face in a video

- Focus on the face, check lighting conditions, and confirm if the person is correctly identified

- Pick unique features like eyes, nose, and so on

- Compare unique features with the training dataset

4.1.2. First-time Registration (Data Collection and storage)

We created a directory to store all the images. Every time the user starts writing their name, a directory gets automatically created inside the images directory, with the person's name being recorded into the system. This process is rapid, and even a second pause leads to the creation of the directory. Once the directory is created, ten images are automatically stored in the system. All the images are collected and stored in about 3 or 4 seconds.

Only one image is required to create the face encoding using Adam Geitgey's library [9]. Despite that, we are going ahead with this approach so that it gives us and any other person who wants to build upon this project the freedom to not only choose one-shot learning-based methods for face recognition but also try different approaches. The code for this is private in its complete form.

4.1.3. Body Temperature Sensing on Raspberry Pi

We have connected an infrared sensor with the Raspberry Pi. This sensor constantly detects the temperature; we can view it on Raspberry Pi's command line. The temperatures are in degrees centigrade. There are Python packages available to help achieve this. We have used smbus2, PyMLX90614 v.0.0.3, gpiozero, and RPi.GPIO.

4.1.4. Maintaining and Viewing the database

We have created a database using MongoDB to store the names, dates, and times of new records and anyone who visits the housing society [10]. The visitor could be a resident, a frequent visitor, or a nonresident is shown in figure 4.
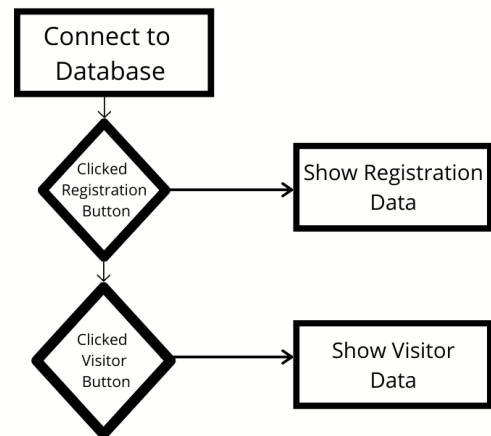
Figure 4: View Database

4.1.5. Sending Report via Email

We have used the SendGrid API, which is more secure than the SMTP client python package. The SendGrid API is also based on the Simple Mail Transfer Protocol (SMTP) principle. The difference is that the Python package required lowering the security of the receiver's GMail Account. In contrast, SendGrid authenticates and verifies the sender, and there is no action required from the receiver to be able to receive an email [11]. The Sendgrid mail flow is shown in figure 5.

Figure 5: Sendgrid Mail Flow

The content sent via email is a dataframe generated from the MongoDB Database that is converted into the Hypertext

Markup Language.

The emails are then scheduled using Python's schedule package. The notification is shown in figure 6.

Figure 6: Email Notification

4.2. Materials

Software:

1. MongoDB (Database) [12]

2. Python (Programming Language) [13]

3. Streamlit (Web Framework) [14]

4. SendGrid API (Email) [15]

5. Remote Desktop Connection (Connecting Laptop with Raspberry PI)

Hardware:
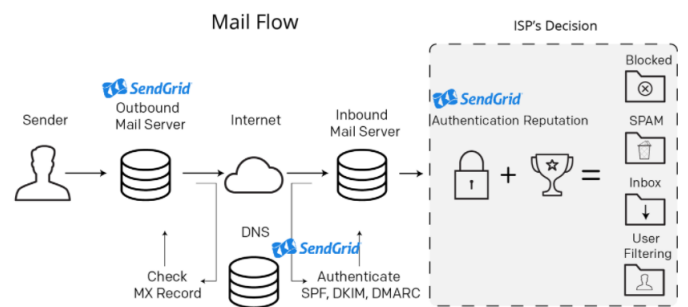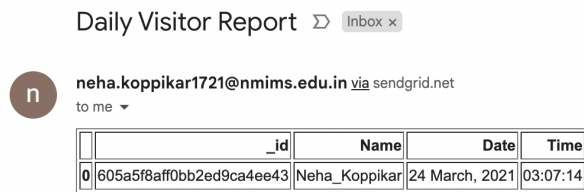
1. Raspberry PI 4 Model B (4GB)

2. Raspberry PI 5MP Camera Board Module

3. LED Bulbs (Red, Yellow, Green)

4. 1 kilo ohm resistors

5. Breadboard

6. Infrared Temperature Sensor GY-906 MLX90614

7. Female to Female Wires (Infrared Sensor and Raspberry Pi Connections)

8. Male to Female wires (LEDs and resistors)

9. BIS 3 Amps Charger, USB C Cable

10. Ethernet Cable

4.3. Application walk trough

4.3.1. First-Time Registration

How it works:

This page of the application is responsible for the initial data collection. This is where the details the following details are collected:

1. First Name

2. Last Name

3. Images for facial recognition

4. Which category does the person fall under? (Resident, Non-Resident, Frequenter)

The resulting page is shown in the figure 7.
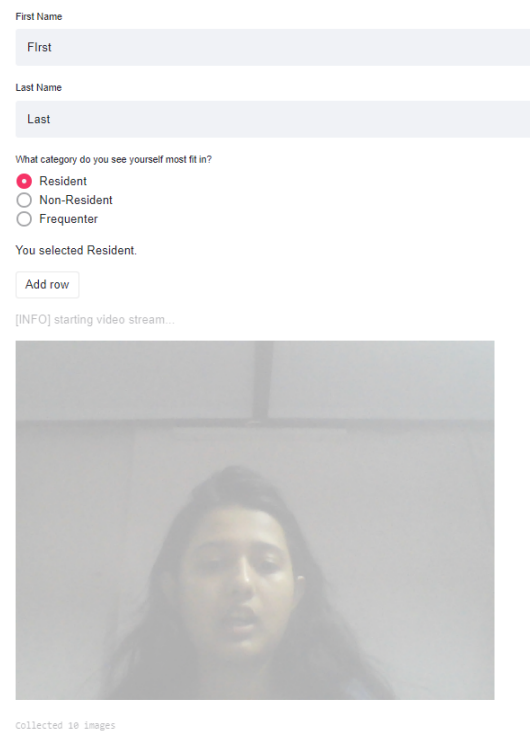
Figure 7: Registration Page - Screenshot

When anyone starts typing in the "First Name" blank, the system is ready to make a directory based on the input collected from the registration page. The person organizing the records has to be quick in typing as even a second of a pause leads to the directory being created, and ten images automatically get clicked and stored in the new directory, and it gets printed on the screen that ten images have been collected.

Due to the pause issue, this page also has an "Add row" button under the category radio option so that the registration record of names and categories gets correctly stored in the database. This can also help in removing the directories that are not required.

Dependencies

Python packages used:

1. Streamlit (streamlit) [14]

2. OpenCV (cv2) [16]

3. Pandas (pandas) [17]

4. Time (time)

5. Datetime (datetime)

6. PyMongo (pymongo) [18]

7. OS (os)

8. Sendrgid API

4.3.2. Face-Recognition

How it works

The camera detects a person, compares the faces with the face embedding [9], and predicts to recognize the person if it is confident more than 60 percent [19].

As soon as the face is recognized, the name, date, and time get automatically stored in the database. This is the other data collection component of the application. The resulting page is shown in the figure 8

Figure 8: Face Recognition Page - Screenshot

Dependencies

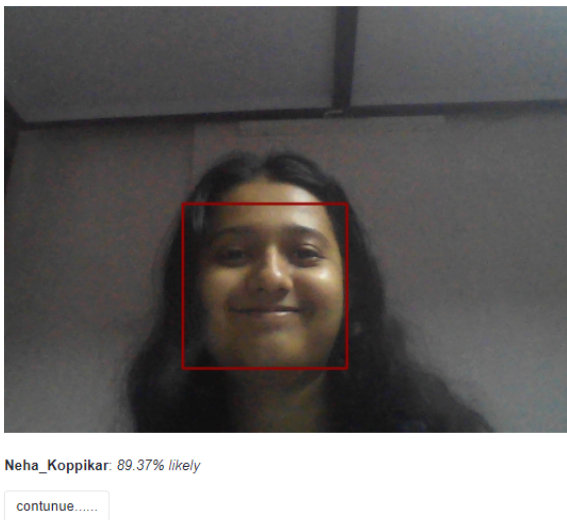Python Packages used:

1. Streamlit (streamlit) [14]

2. OpenCV (cv2) [16]

3. Face Recognition (face-recognition) [20]

4. Dlib-ml: A Machine Learning Toolkit [21]

5. Pandas (pandas) [17]

6. Numpy (numpy) [22]

7. Pickle (pickle)

8. Datetime (datetime)

9. PyMongo (pymongo) [18]

4.3.3. Viewing Database

Why this feature: At times, the maintainer may want to see if the application is working correctly or not. This feature helps check that. The maintainer will remember the recent entries anyway as the maintainer is most probably a security who is habituated to keeping track of these things. The maintainer can view the database and compare it with their memory. Since the data cannot be edited from the application, the data is not compromised.

How it works:

All the data stored in the database is accessed as a data frame and displayed on the screen. The visitor data is shown in figure 9.

Figure 9: Visitor Database - Screenshot

4.3.4. Sending Emails

Why this feature:

While the application will be used mainly by the security guards, the society's secretary is also answerable in the case of an anomaly. That is why there is a requirement to keep a check on what is happening, and checking the system now and then can be inconvenient to both the maintainer of the application and the secretary. This feature helps solve this problem by emailing a report to the secretary. For this purpose, we have used the SendGrid API [15].

How it works:

The database stores all the face-recognition data as a data frame and this data frame is sent as a report to the receiver of the email, which is preferably the secretary of the society. The resulting email is shown figure 10.

Figure 10: Email - Screenshot

Dependencies

Python Packages used:

1. SendGrid (sendgrid) [15]

2. Schedule (schedule)

3. Datetime (datetime)

4. Pandas (pandas) [17]

5. PyMongo (pymongo) [18]

4.3.5. Raspberry Pi

Initial Set up:

1. Install Raspbian OS into SD card

2. Insert the SD card

3. Connect Raspberry Pi to PC [23]

4. Find the IP Address of the Raspberry Pi

5. Connect the laptop with the Raspberry Pi remotely [24]

The above steps are generic.

Important Changes from the web application:

1. The camera is accessed from the laptop using the OpenCV Python package. The picamera is accessed from the Raspberry Pi using the imutils [25] python package.

2. There are dependency issues in installing MongoDB into Raspberry Pi locally. Alternatively, Ubuntu provides an unofficial Mongodb package.

Schematic Representation:

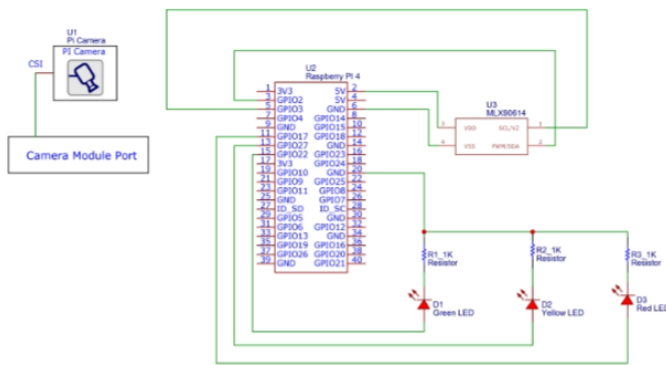The Raspberry Pi Schematic Representation is shown in the figure 11.

Figure 11: Raspberry Pi Schematic Representation

4.3.6. Body Temperature Sensing

How it works: In this project, we use a contactless Infrared (IR) Digital Temperature Sensor called MLX90614. This sensor makes use of IR rays to measure the temperature of a person or object without any physical contact with it. The communication between the sensor and Raspberry Pi 4 is established using the I2C protocol [26]. The severity of the sensed temperature is shown via an LED lighting system inspired by a traffic signal. The system is connected to the microcontroller with the help of wires. The working of the temperature sensing system can be summarized in the following points:

1. The person or object whose temperature is to be measured is brought in the range of the temperature sensor.

2. The infrared sensor senses the temperature and returns it to the Raspberry Pi 4.

3. With the help of the LED system, we can identify a person's temperature in three categories: Normal, Borderline, and High.

4. When the temperature sensed is below 37 degrees centigrade, the Green LED turns ON, indicating Normal temperature.

5. When the temperature sensed is between 37 degrees centigrade and 38 degrees centigrade, the Yellow LED turns ON, indicating Borderline temperature.

6. When the temperature sensed is above 38 degrees centigrade, the Red LED alone turns ON, indicating the temperature to be High.

Dependencies:

1. smbus2

2. PyMLX90614 0.0.3

3. gpiozero

4. RPi.GPIO

5. Alternatives considered

5.1. Frameworks

1. Django (Python-Based Web Framework) [27]

2. Flask (Python-Based Web Framework) [27]

3. React (JavaScript-Based Web Framework)

5.2. Database

1. MySQL

2. PostgreSQL

5.3. Sending Emails

Python's SMTP client can also be used. The primary issue is that it requires a few settings in our GMail accounts, which lowers the security level and increases the risk of hacking.

5.4. Accessing Raspberry Pi

We have used Remote Desktop Connection. VNC Viewer can also be used.

5.5. Challenges Faced

1. Remote Desktop Connection with the Raspberry is lost after about an hour.

2. Integrating the entire application seamlessly.

3. When we started, we were not well-versed with any framework, including Flask.

4. The issue that we faced with the flask was that we were not able to stream the input from the webcam for the registration page and the face recognition page at the same time. (Navigation bar used). That is why we switched to Streamlit.

5.6. Limitations of Proposed System

1. Cannot toggle between the database option when running the application file. To view the database, the file has to be run separately.

2. Streamlit Installation into Raspberry Pi was solved by downgrading the version [23].

6. Discussion

Our experiment shows that even though biometrics is essential in a security or monitoring system, what improves it even more is a email report notification system to be in place. This project showcases a smart monitoring system that stores images, fine-tunes a face-recognition model using one-shot learning, stores the images and personal information of a person, and sends email reports to a responsible point of contact daily. The web application also allows viewing the database that cannot be edited or changed, thereby acting as a security feature.

There are a few limitations to this research project, though. A better security design or mechanism can be built that not only stores and sends data but also alerts the responsible point of contact in case of an anomaly situation. This application cannot be scaled up or down quickly as it is built on-prem. Therefore, making it on a cloud computing platform could have been a better choice and scope for future research.

7. Limitation

A few limitations of the application are:

1. The hardware disconnects from the software sometimes.

2. Considering the sensitivity of the data we are using, a security system to ensure data privacy is not in place.

8. Future Scope

1. Adding the feature to detect mask positioning [6].

2. Make the application more user-friendly

3. The application has to be made spoof-proof as a layer of security [28].

4. Temperature cannot be backtracked. Figure out how to backtrack the temperature and link that with the person into the database efficiently.

5. If this application is deployed on the cloud. It will help with scaling the application.

6. Face Recognition frameworks like FaceNet and Open-Face can be used.

7. A system to ensure the security and privacy of the data in the future.

9. Result and Conclusion

We are glad that the application is working, and we learned a lot. We learned about frameworks in Python, ways to send an email, schedule an email, face recognition, and manage databases, among many others. Though there are a lot of places where this application can be improved, it should be a good starting point for someone who wants to work on this application at a bigger level. In the future, we can use a better face-recognition algorithm, a cloud computing platform, or apply action recognition to identify harmful actions and capture the person's name for enhanced security.

Declaration of competing interest The authors declare that they have no known competing financial interests or personal relationships that could have appeared to influence the work reported in this paper.

References

[1] D. R.S, "Attendance authentication system using face recognition", *Journal of Advanced Research in Dynamical and Control Systems*, vol. 12, pp. 1235–1248, 2020, doi:10.5373/JARDCS/V12SP4/20201599.

[2] T. Sollu, Alamsyah, M. Bachtiar, B. Bontong, "Monitoring system heartbeat and body temperature using raspberry pi", *E3S Web of Conferences*, vol. 73, p. 12003, 2018, doi:10.1051/e3sconf/20187312003.

[3] A. Cabani, K. Hammoudi, H. Benhabiles, M. Melkemi, "Maskedface-net – a dataset of correctly/incorrectly masked face images in the context of covid-19", *Smart Health*, 2020, doi:https://doi.org/10.1016/j.smhl.2020.100144.

[4] F. Schroff, D. Kalenichenko, J. Philbin.

[5] T. Benoit-Cattin, D. Velasco-Montero, J. Fernández-Berni, "Impact of thermal throttling on long-term visual inference in a cpu-based edge device", 2020.

[6] M. Saifuzzaman, A. Hossain, N. Nessa, F. Nur, "Smart security for an organization based on iot", *International Journal of Computer Applications*, vol. 165, pp. 33–38, 2017, doi:10.5120/ijca2017913982.

[7] T. Gunawan, M. Gani, F. Rahman, M. Kartiwi, "Development of face recognition on raspberry pi for security enhancement of smart home system", *Indonesian Journal of Electrical Engineering and Informatics*, vol. 5, pp. 317–325, 2017, doi:10.11591/ijeei.v5i4.361.

[8] K. Naik, "Deep-learning-face-recognition", 2020.

[9] A. Geitgey, "Save face encodings", 2018.

[10] "miscmonggodb raspberry pi installation, unable to locate package mongodb-org", .

[11] S. AGNEW, "How to send emails in python with sendgrid,", 2019.

[12] K. P. R. Eliot Horowitz, Dwight Merriman, "Mongodb", 2009.

[13] G. Van Rossum, F. L. Drake Jr, *Python tutorial*, Centrum voor Wiskunde en Informatica Amsterdam, The Netherlands, 1995.

[14] C. K. F. A. J. A. J. R. J. M. N. S. T. R. Ashish Shukla, Charly Wargnier, "Streamlit - the fastest way to build and share data apps", 2019.

[15] J. L. Isaac Saldana, T. Jenkins, "Sendgrid", 2009.

[16] I. Intel Corporation, Willow Garage, "Opencv", 2000.

[17] W. McKinney, "Pandas", 2008.

[18] A. Sottile, "Pymongo", 2017.

[19] Nyahua, "Face recognition from webcam using streamlit", 2020.

[20] A. Geitgey, "Face recognition", 2017.

[21] D. E. King, "Dlib-ml: A machine learning toolkit", *Journal of Machine Learning Research*, vol. 10, pp. 1755–1758, 2009.

[22] T. Oliphan, "Numpy - the fundamental package for scientific computing with python.", 2006.

[23] E. Krupesh, "How to connect raspberry pi to pc (smartphone hotspot, no lan cable)", 2019.

[24] educ8s.tv, "Raspberry pi remote desktop connection", 2019.

[25] "I need this code to use the pi camera and not a webcam", .

[26] "Mlx90614 non-contact ir temperature sensor", .

[27] S. W. Adrian Holovaty, "Django (web framework)", 2005.

[28] S. Kumar, S. Singh, J. Kumar, "A comparative study on face spoofing attacks", "2017 International Conference on Computing, Communication and Automation (ICCCA)", pp. 1104–1108, 2017, doi: 10.1109/CCAA.2017.8229961.

Quantum Machine Learning on Remote Sensing Data Classification

Yi Liu[1] , Wendy Wang*[2] , Haibo Wang[3] , Bahram Alidaee[4]

[1] University of Massachusetts Dartmouth, Department of Computer and Information Science, Dartmouth, MA 02747, USA

[2] University of North Alabama, Computer Sciences and Information Systems, Florence, AL 35632, USA

[3] Texas A&M International University, Division of International Business and Technology Studies, Laredo, TX 78041, USA

[4] University of Mississippi, Department of Marketing, Oxford, MS 38677, USA

* Corresponding author: Wendy Wang, Florence, Alabama 35632, (256)-765-5273 & hwang21@una.edu

ABSTRACT: Information extracted from remote sensing data can be applied to monitor the business and natural environments of a geographic area. Although a wide range of classical machine learning techniques have been utilized to obtain such information, their performance differs greatly in classification accuracy. In this study, we aim to examine whether quantum-enhanced machine learning can improve the performance of classical machine learning algorithms in binary classifications of satellite remote sensing data. Using 16 pre-labeled datasets, we apply Support Vector Machine-quantum annealing solver (SVM-QA) - a type of quantum machine learning algorithm, with optimized (Gamma) value on the task of image classification and compare its results with the top performers of classical machine learning algorithms. The results show that in 10 out of 16 datasets, the hyper parameterized SVM-QA classifier outperforms the best classical machine learning algorithms in terms of classification accuracy. The findings suggest the potentiality of quantum computing in remote sensing. This study contributes to the literature of remote sensing image data classification and applications of quantum machine learning for problem solving.

KEYWORDS: Machine Learning, Remote Sensing Data Classification, Support Vector Machine, Classical Machine Learning

1. Introduction

Remote sensing is a method of gathering data about a particular object or a geographical area without physical contact. It can quickly provide static or dynamic geospatial data with various scales and resolutions. Such datasets provide insights beneficial for society and the natural environment.

Remote sensing datasets play an important role in many big data applications, e.g., spatial analysis, earth observation modeling, urban planning, and prompt response to rapid changes in demographic, economic, and technological landscapes [1-4]. Massive geospatial data have been collected from a wide range of sources, such as satellites [5], mobile devices [6], and aerial photography [7] etc. It is essential to extract valuable information from these remote sensing data using computationally efficient techniques [8-10].

Remote sensing data classification aims to label images with a semantic class, typically involving pattern identification and classification based on content within given datasets [11]. Because of machine learning's capacity of handling high-dimensional data and mapping classes with complex characteristics, it has been applied extensively to a wide range of remote sensing imagery classification - for example, delineation of cadastral boundaries [12], aero-images of the roof damage caused by earthquake in Japan [13], and urban land use and land mapping in France [1]. Although machine learning applications have demonstrated better accuracy than those using traditional parametric classifiers [14], the overall classification accuracy of the top algorithms is far from satisfactory [15].

There are several issues that hinder breakthroughs in remote sensing data classification: the complexity and sheer volume of remote sensing geospatial data [9-10], difficulties in distinguishing intra-class diversity and

inter-class similarity, variations in scene images at different scales, and the challenge of processing scenes with multiple objects, among others [11]. With the development of advanced machine learning, techniques such as deep learning have been deployed to address these data-intensive problems, such trend makes it imperative to have more powerful computing resources and extensive training datasets [8]. The escalating demand for exceptional computing power and the shortage of large-scale datasets due to the labor-intensive process of creating them, have become a bottleneck for remote sensing data processing [11, 16]. In addition, the use of different datasets and procedures in various studies has often led to conflicting and incomparable findings. As a result, many classification studies have yielded contradictory conclusions in identifying the best performers, making it laborious to select the optimum machine learning algorithm for a specific classification task.

Quantum computing is a multidisciplinary field that applies quantum mechanics to provide solutions that are either impossible or computationally too expensive using traditional methods. It is among the latest rapidly advancing technological breakthroughs and provides a potentially effective alternative to address issues in remote sensing [8]. Although still in its preliminary stage, quantum computing can conceptually solve optimization processes that are core to many machine learning and deep learning algorithms expeditiously.

Moving beyond the effort of selecting an optimum classifier from traditional machine learning algorithms, this study approaches remote sensing data classification from the paradigm of quantum computing and compares how it performs with classical machine learning. In this study, we aim to explore whether quantum machine learning delivers higher prediction accuracy than classical machine learning for binary classification of remote sensing images.

The rest of the paper is organized as follows: Section 2 provides an overview of the extant literature on quantum machine learning particularly on how support vector machine-quantum annealing (SVM-QA) solver - a type of quantum machine learning annealing algorithm has been applied in the analysis of remote sensing data. Section 3 describes the characteristics of datasets used and explains how the best performing SVM-QA is selected for the comparison with the top-performing classical machine learning algorithms in terms of accuracy. Sections 4 and 5 present and evaluate the results of this study, and section 6 concludes this study and discusses future work.

2. Related Work

2.1. Classical Support Vector Machine (SVM) and Support Vector Machine - Quantum Annealing (SVM-QA)

Kernel-based Support Vector Machine is one of the most popular and robust supervised machine learning algorithms for classification and regression [17]. It conducts classification by constructing an optimal hyperplane that separates labeled training data into different groups with maximum distance. Hyperplanes are boundaries that separate data into two different classes, with data points belonging to one class tending to fall on the same side of the hyperplane. Support Vector Machine classifiers categorize new data into different groups using these hyperplanes [18].

Support Vector Machine based classifiers have found applications in wide ranges of areas such as electrocardiogram (ECG) abnormality detection [19], water waste treatment [20], network security attack detection [21], and more. Its popularity can be attributed to the ability to handle high-dimensional and complex data, even for unstructured and semi-structured data, such as text and images.

Support Vector Machine also has other advantages. For example, Support Vector Machine based classifiers do not have much divergence over small variations in training datasets, so they are more reliable and have the advantage of a low risk for overfitting. In addition, SVMs do not require extensive training data compared to deep Learning algorithms and can be used when only limited training data is available [17].

Depending on the characteristics of datasets and features, SVM can implement either linear or nonlinear classifiers. Linear SVM Classifier (SVC) is suitable for classifying datasets with separable linear features, while nonlinear SVC is better fitted for datasets with nonlinear features. Nonlinear features are often transformed to linear ones since linear SVC is easier to implement. The transformation is called *kernel trick*, which helps finding the optimal hyperplane easily. The robustness of SVM comes from kernel trick, SVC can address complicated problems with the right kernel function. However, due to the computational complexity to find the solution $O(n^3)$ where n is the number of training data points, SVM classifiers are typically not used on very large datasets because of the extensive training time required [22]. Section 2 illustrates how the kernel trick is performed mathematically.

Quantum computing is an exciting interdisciplinary research area aimed at solving complex problems that classical computers are too slow to handle [23]. Since quantum computing uses quantum bits, or qubits which has more than one state simultaneously, whereas classical computers employ bits which have either the state of 1 or 0, it is significantly more cost efficient than their classical counterparts [10]. The increasing attention from both research and industry communities on quantum computing and machine learning has fueled the trend of

Quantum Machine Learning (QML) which combines the capabilities of both [10, 17]. Quantum Machine learning is a sub discipline of Quantum Artificial Intelligence (QAI), seeking to build quantum enhanced machine learning algorithms or novel methods which can improve the performance of classical algorithms [10, 24]. By taking advantage of qubits, quantum operations, and quantum computers processing capabilities, Quantum Machine learning can theoretically take quantum leap in the processing speed compared to classical machine learning. This makes QML effective in finding solutions to problems considered unsolvable in the classical computing environment. QML has been shown to overcome the issue of slow convergence and training when implemented in a quantum computing platform [23]. Because of Support Vector Machine's advantages in robustness and scalability in processing complex data, we have chosen to apply quantum computing to satisfy the computation demand of machine learning in terms of time. The next section provides details on how SVM can be enhanced by quantum annealing and its formulation.

2.2. Formulation of Support Vector Machine – Quantum Annealing (SVM-QA)

Constructing SVM kernel functions on nonlinear classifiers is very tedious, it is time consuming even when the datasets are not big. Applying quadratic infeasibility penalties as an alternative for imposing constraints explicitly, this study has developed a general quadratic constrained model for SVM and recast it in the form of binary quadratic programming problem. This SVM-QA formulation can be solved by a number of quantum annealing solvers [25]. In the SVM-QA model, the support vector classifier can use the typical Radial Basis Function (RBF) kernel: $RBF(x_n, x_m) = e^{-\lambda\|x_n - x_m\|^2}$. The λ (lambda) value is the only adjustable parameter in the kernel function and plays an important role in the model's performance.

Since Kernel-based machine learning algorithms, such as support vector machines (SVMs), can experience prolonged processing times when dealing with large-scale data, to address this issue, we first transform the radial basis function (RBF) kernel of the SVM into a quadratic integer programming model, then use binary transformation to make this model compatible with quantum computing platforms. For a data set with m attributes and N observations, the binary value of the response variable (classifiers) for i^{th} observation y_i is $y_i \in \{-1, +1\}$; vector $X \in \mathbb{R}^{N \times m}$ representing the training data, and vector $Y \in \{-1, +1\}^N$, the support vector classifier in the decision functions that formulates the hyperplane is identified by coefficients $a \in \mathbb{R}^m$ and bias $b \in \mathbb{R}$:

$$\min_{a,b} \frac{1}{2}\|a\|^2 \quad \text{s.t.} \quad y_i(a^T x_i + b) \geq 1, \forall i = 1, 2, \cdots, N \qquad (1)$$

Decision function (1) is the convex quadratic programming problem. The linear constraints in (1) can be transformed to the objective function by a vector of Lagrangian multipliers:

$$\gamma = [\gamma_1, \ldots, \gamma_N]^T \text{ and } \gamma_i \geq 0, \forall i = 1, \cdots, N$$

$$\mathcal{L}(a, b, \gamma) = \frac{1}{2}\|a\|^2 - \sum_{i=1}^{N} \gamma_i [y_i(a^T x_i + b) - 1] \qquad (2)$$

The Lagrangian problem (2) can be solved by Karush-Kuhn-Tucker conditions [26] by setting both the gradient of (2) with respect to a and the derivative of (2) with respect to b to zero. This can be expressed as follows:

$$\nabla_a \mathcal{L}(a, b, \gamma) = a - \sum_{i=1}^{N} \gamma_i y_i x_i = 0 \qquad (3)$$

$$\frac{\partial \mathcal{L}(a,b,\gamma)}{\partial b} = -\sum_{i=1}^{N} \gamma_i y_i = 0 \qquad (4)$$

By substituting (3) and (4) in (2), we get the Lagrangian problem (5).

$$\mathcal{L}(\gamma) = \sum_{i=1}^{N} \gamma_i - \frac{1}{2}\sum_{i=1}^{N}\sum_{j=1}^{N} \gamma_i \gamma_j y_i y_j x_i x_j \qquad (5)$$

x_i represents the values of predictor variables, and y_i the value of the classifier for observation i. The decision function of the SVM can be formulated as a problem of maximizing (5) subject to the constraints of the decision variable $\gamma_i \geq 0, \forall i = 1, \cdots, N$, given in compact form in (6).

$$\max_{\gamma} \mathcal{L}(\gamma) = \gamma^T 1_N - \frac{1}{2}\gamma^T(XX^T \odot YY^T)\gamma, \quad \gamma \geq 0_N \qquad (6)$$

The decision variables in (5) and (6) are continuous. Following [25] and introducing precision vector of P and binary variables $\hat{\gamma}$, we can convert decision variables γ_i, for $i = 1, \ldots, N$, into the sum of binary variables. This is the same as $\hat{\gamma}P$, thus,

$$P = [p_1, \ldots, p_K]$$

$$P = 1_N \otimes P^T$$

$$1_N \otimes P^T = \begin{bmatrix} p_1 & \cdots & p_K \\ \vdots & \cdots & \vdots \\ p_1 & \cdots & p_K \end{bmatrix}$$

$$\hat{\gamma} = [\hat{\gamma}_{11}, \ldots, \hat{\gamma}_{1K}, \ldots, \hat{\gamma}_{N1}, \ldots, \hat{\gamma}_{NK}]$$

$$\hat{\gamma} = \begin{bmatrix} \hat{\gamma}_{11} & \cdots & \hat{\gamma}_{1K} \\ \vdots & \cdots & \vdots \\ \hat{\gamma}_{N1} & \cdots & \hat{\gamma}_{NK} \end{bmatrix}$$

Now we have

$$\sum_{k=1}^{K} \hat{\gamma}_{ik} p_k, \quad \forall i = 1, 2, \cdots, N \qquad (7)$$

where $\hat{\gamma}_{ik}$ corresponds to the element of Lagrangian multipliers vector γ, and P_k is an element of k-dimensional precision vector of P, which is used to convert the continuous variable γ_i into a sum of binary variables. In (7), a combination of values of $p_k, \forall k = 1, \ldots, K$, may be chosen. This means several $\hat{\gamma}_{ik}, \forall k = 1, \ldots, K$, may be equal to 1.

1_N and 0_N represent N-dimensional vectors of 1 and 0, the $\odot$ refers to the element-wise multiplication operation in equation (6). In (5), γ_i, γ_j are continuous variables. By applying the binary expansion method with the power of 2, the continuous variable γ_i can be transformed into a sum of binary variables with a K-dimensional precision vector $P = [p_1, p_2, \cdots, p_K]^T$, where $P = 1_N \otimes P^T$ and $\otimes$ is the tensor product for two vectors. K is the researcher-set value for the desired precision. When K value is set larger, the size of Q matrix will grow accordingly, which would lead to longer computing time. Based on our experience, a value between 3 to 5 for K would be sufficient to evaluate the objective function with continuous variables and its binary expansion representation. The decision variable γ_i can be transformed by K binary variables $\hat{\gamma}_{ik}$: $\gamma_i = \sum_{k=1}^{K} \hat{\gamma}_{ik} \, p_K \quad \forall i = 1,2,\cdots, N$ and $\sum_{k=1}^{K} \hat{\gamma}_{ik} \leq 1, \forall i = 1, \ldots, N$. Then the binary expansion of vector of Lagrangian multipliers γ is the following, given:

$$\gamma = P\hat{\gamma} \quad \text{where } \hat{\gamma} = [\hat{\gamma}_{11}, \cdots \hat{\gamma}_{1K}, \cdots \hat{\gamma}_{NK}]^T \tag{8}$$

With the binary expansion of γ in (8), the problem in (6) becomes:

$$\max_{\hat{\gamma} \in \mathbb{B}^{NK}} \mathcal{L}(\hat{\gamma}) = \hat{\gamma}^T P^T 1_N - \frac{1}{2}\hat{\gamma}^T P^T (XX^T \odot YY^T)P\hat{\gamma} \tag{9}$$

The problem in (9) then has the form of Quadratic Unconstrained Binary Optimization (QUBO) [27]

$$\max_{\hat{\gamma} \in \mathbb{B}^{NK}} \mathcal{L}(\hat{\gamma}) = \hat{\gamma}^T D - \frac{1}{2}\hat{\gamma}^T A\hat{\gamma} \tag{10}$$

where $D = P^T 1_N$ and $A = P^T(XX^T \odot YY^T)P$.

Thus, in lieu of placing constraints, we apply Lagrangian multipliers and binary expansion method to first develop a general quadratic constrained programming model for SVM in (1), and the recast in the form of quadratic unconstrained programming (QUP) model in (9). The transformed SVM model formulation can be solved using several quantum annealing solvers [17].

2.3. Quantum Machine Learning (QML) and Remote Sensing

Quantum annealing algorithms are designed to process qubits, which are quantum data that can operate in a quantum computing environment. Since many classical data are multi-dimensional and difficult to map into qubit data [23, 28], the range of problems that quantum annealing algorithms can address is limited, and many proposed solutions are still in the conceptual stage. Regardless, due to the quantum computing's capabilities, it is expected to eventually play an important role in solving complicated problems [8, 10, 17], one of which is the classification of remote sensing satellite images. Applications of Quantum Machine Learning in remote sensing data processing are relatively few and are mostly used as proof of concept [8, 23, 28].

Current literature of QML applications primarily focuses on the fields of earth and space sciences, for example, there have been experiments with quantum neural networks using reference earth observation data, exploration of methods to directly map certain types of earth observation data to quantum data [28], and investigations into the application of quantum computing in space exploration [29]. Since Support Vector Machine is a popular algorithm for supervised classification tasks, capable of processing complex data such as text and images, and requiring relatively small training data [23], it is the algorithm of choice in QML application of processing remote sensing image data when the labeled datasets are limited [23], also used in this study.

3. Methods

3.1 Datasets

This study uses the datasets from HyperLabelMe [16], a web platform that provides pre-labeled datasets for benchmarking remote sensing image classifiers. Motivated by the goal of providing benchmarking data and increasing comparability of study results, the Image and Signal Processing (ISP) group at the Universitat de Val`encia has collected, harmonized, and shared a big database of forty-three text-based datasets harmonized from multispectral and hyperspectral remote sensing images. Each dataset consists of an n by m matrix of numerical values. In this study, sixteen datasets with binary classification classes are selected for testing and comparison purposes. Researchers can test their classification algorithms using these datasets and share their results on this site to benchmark other studies.

In this study, we have implemented quantum annealing enhanced Support Vector Machine, a quantum-enhanced machine learning algorithm, and applied it to 16 sets of hyperspectral remote sensing datasets from HypberLabelMe platform. Table 1 describes the characteristics of the datasets used in this study which includes their names, sensors used, and dataset scales etc. 9% of the instances in each dataset are labeled. For the unsupervised and semi-supervised learning approaches, the instances are fed to the algorithms without labels.

Table 1: Dataset Description

Data Name & Sensor	Row	Column	Bands	Labeled	Unlabeled
Naples95 (Landsat)	200	200	7	500	5,000
Naples99 (Landsat)	200	200	7	500	5,000
Naples99(full) (Landsst)	400	400	7	500	5,000
Mexico (Landsat)	360	512	2	500	5,000
Barrax (MERIS)	1,247	1,153	13	500	5,000

France (MERIS)	2,399	2,241	13	500	5,000
Abracos (MERIS)	321	490	15	500	5,000
Ascension Island (MERIS)	321	490	15	500	5,000
Azores (MERIS)	321	493	15	500	5,000
Barcelona (MERIS)	321	493	15	500	5,000
Capo Verde (MERIS)	321	492	15	500	5,000
Longyearbyen (MERIS)	321	493	15	500	5,000
Mongu (MERIS)	321	489	15	500	5,000
Ouagadougou (MERIS)	209	492	15	500	5,000
Rome95 (Landsat)	200	200	7	500	5,000
Rome99 (Landsat)	200	200	7	500	5,000

3.2 Classification Workflow

Fig 1 illustrates the workflow of the remote sensing image classification used in this study.
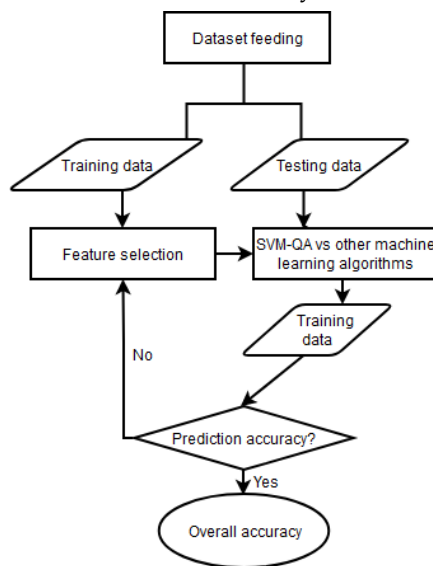

Figure 1: Classification workflow

The input dataset is split into a training set and a testing set. This study uses 80% of each input dataset which is a commonly used ratio as the training set and the remaining 20% as the testing set. Since there are variables that do not contribute to the prediction accuracy of the model, and some even reduce the prediction accuracy, recursive feature elimination (RFE) [30] is used to remove such attributes while constructing prediction models. This process is captured in the step feature selection to the training data. The kernel functions of SVM formulated and solved by quantum annealing solvers are used in classifications.

3.3 Evaluation process

To investigate whether quantum machine learning can deliver consistent and reliable results, this study has included two sets of evaluations. In one evaluation, we have selected benchmarks from our own tests using sixteen supervised, semi-supervised, and unsupervised machine learning algorithms. In another test, the benchmarks have been identified from evaluation results of seven traditional machine learning algorithms shared by other researchers on HyberLabelme platform. To improve the generalization of the findings, this study has taken the recommendation of including multiple classifiers for a specific classification task in the evaluation [14-15]. In both rounds of evaluations, only the algorithm that has the best AUROC value for every dataset is identified for that group, and has been used for benchmark purpose. Thus, quantum machine learning is compared against only the best performer for each of the 16 datasets in two rounds of evaluations. This approach would demonstrate whether quantum machine learning delivers consistent results, and having two evaluations has also increased the reliability of the study.

Table 2 has listed all eighteen algorithms used as benchmarks in the two rounds of evaluations. The first set compares the results of SVM-QA with the best results posted on HyperLabelMe using seven classical machine learning algorithms: SVM, random forest (RF), extreme learning machines (ELM), k-nearest neighbor (KNN), linear discriminant analysis (LDA), logistics regression (LR), and fast and deep deformation approximations (FDDA). The results from HyperLabelMe were posted and made available for public access by other researchers. The second set compares the results of SVM-QA with the best results from our own implementation experiments using sixteen out of all eighteen methods listed in Table 2 (excluding Fast and deep deformation approximations and Extreme learning machines used in the first evaluation).

Table 2: Machine Learning Algorithms Used

Type	Machine Learning Algorithms
Unsupervised	Fast and deep deformation approximations (FDDA) [31]
	K-nearest neighbor (KNN) [32]
Semi-supervised	Ensemble method-regression trees (RT) [33] and logistics regression (LR)
Supervised	Adaptive Boosting (AdaBoost) [34]
	Balanced bagging [35]
	Complement naive bayes (NB) [36]
	Convolutional neural networks [37]
	Copula-Based Outlier Detection (COPOD) [38]
	Ensemble method-random forest (RF) [39] and RUSBoost [40]
	Extreme learning machines (ELM) [41]
	eXtreme gradient boosting (XGBoost) [42]
	Linear discriminant analysis (LDA) [43]

Light gradient boosting machine (LightGBM) [44]
Logistics regression (LR) [45]
Neural Networks-multilayered perceptrons (MLP) [46]
Random forest (RF) [39]
Support vector machines (SVM) [47]
v-Support Vector Machines (NuSVM) [48]

Python 3.8 and standard packages from the SciKit Learn library are used in coding the 16 classical machine learning algorithms, and D-Wave quantum annealing solver is applied to solve the SVM-QA model.

4. Results

Identification of the optimal γ value is important for the QA module of SVM to achieve good performance in accuracy. To identify the most appropriate one, we have examined the impact of three commonly used γ values (0.125, 0.25, and 0.5) as SVM hyperparameters on the accuracy performance of SVM-QA.

There are primarily two ways to measure the classification accuracy of the models [49]: accuracy and Area Under the Curve of the receiver operating characteristics (AUROC). Accuracy counts how many predictions are correct, whereas AUROC value presents the ratio of true positives to the portion of true negatives (a true positive refers to the case when the model correctly classifies the data, and a true negative occurs when the model correctly identifies the negative class), hence AUROC is more effective in assessing the performance of the models. AUROC has values from 0 to 1, the higher the value, the better the performance. In this study, we use AUROC to measure the performance of the classifiers. The findings indicate that a γ value of 0.125 yields the best accuracy for 10 out of 16 datasets (see Table 3).

Table 3: SVM-QA AUROC with Different γ Settings

Dataset	γ = 0.125	γ = 0.25	γ = 0.5
Naples95	0.997	0.998	0.995
Naples99	0.987	0.981	0.962
Naples99 (full)	0.934	0.919	0.914
Mexico	0.988	0.985	0.983
Barrax	0.986	0.921	0.940
France	0.972	0.972	0.977
Abracos	0.972	0.950	0.876
Ascension Island	0.996	0.991	0.971
Azores	0.994	0.996	0.997
Barcelona	0.968	0.978	0.939
Capo Verde	0.933	0.927	0.863
Longyearbyen	0.868	0.897	0.793
Mongu	0.978	0.980	0.959
Ouagadougou	0.972	0.971	0.971
Rome95	0.960	0.945	0.922
Rome99	0.864	0.843	0.819

The SVM-QA results with the γ value of 0.125 is selected to compare with the best-performing of classical machine learning methods on each of the 16 datasets (see Table 4).

Table 4: SVM-QA vs Best Machine Learning Algorithms

Dataset Name	Best * AUROC[1]	Columns	Class	SVM-QA AUROC	Best ** AUROC[2]
Naples95	0.9674[3]	200	2	**0.997**	0.9943
Naples99	0.9518[5,6]	200	2	**0.987**	0.9827
Naples99(full)	0.8674[1]	400	2	**0.934**	0.9228
Mexico	0.9590[1]	512	2	**0.988**	0.9879
Barrax	0.9678[1]	1,153	2	*0.986*	0.9915
France	0.9856[1]	2,241	2	0.972	0.9711
Abracos	0.9882[4]	490	2	0.972	0.9993
Ascension Island	0.9810[3]	490	2	**0.996**	0.9949
Azores	0.9980[2]	493	2	0.994	0.9981
Barcelona	0.9606[2]	493	2	*0.968*	0.9716
Capo Verde	0.9476[1]	492	2	0.933	0.9232
Longyearbyen	0.9312[3]	493	2	0.868	0.9292
Mongu	0.9714[1]	489	2	0.97	0.9837
Ouagadougou	0.9702[1]	492	2	**0.972**	0.9858
Rome95	0.9025[1]	200	2	**0.960**	0.9421
Rome99	0.8273[1]	200	2	**0.864**	0.8616

Note: AUROC[1] refers to best result posted on HyperLabelMe using machine learning algorithms, numbered based on their performance: 1-SVM, 2-RF, 3-ELM, 4-KNN, 5-LDA, 6-LR, 7-FDD; AUROC[2] refers to best results from our tests with 16 machine learning algorithms.

The performance of the classifiers varies depending on the datasets. To evaluate how QML compares to classical machine learning algorithms and produce more generalizable results, Table 4 presents a comparison of accuracy (AUROC) for SVM-QA with the best classifiers as benchmarks in two evaluations. One set of benchmarks is drawn from the results shared by other researchers on HyperLabelMe (column Best * AUROC[1]), while the other benchmark datasets are based on our own tests (column Best **AUROC[2]).

Figure 2 illustrates the AUROCs obtained by applying SVM-QA on the 16 datasets, while Figure 3 shows the AUROC obtained by applying other 16 machine learning algorithms on the Naples95 dataset. D-Wave solver generates a Q matrix out of 80% of the training data and then randomly selects 50 samples from the matrix for training. The hyperparameters for SVM-QA are set as follows: B = 2, K = 2, x_i = 0, γ = 0.125. Here, B represents the base used for the encoding, K is the number of binary variables used to encode the continuous decision variables, and x_i is the multiplier for the encoding process. The SVM-QA values are highlighted in bold font when they surpass the results of both other researchers' tests shared on HyperLabelMe and our tests. In addition, SVM-QA are highlighted in italics when they exceed HyperLabelMe results but are lower than the ones from our tests.
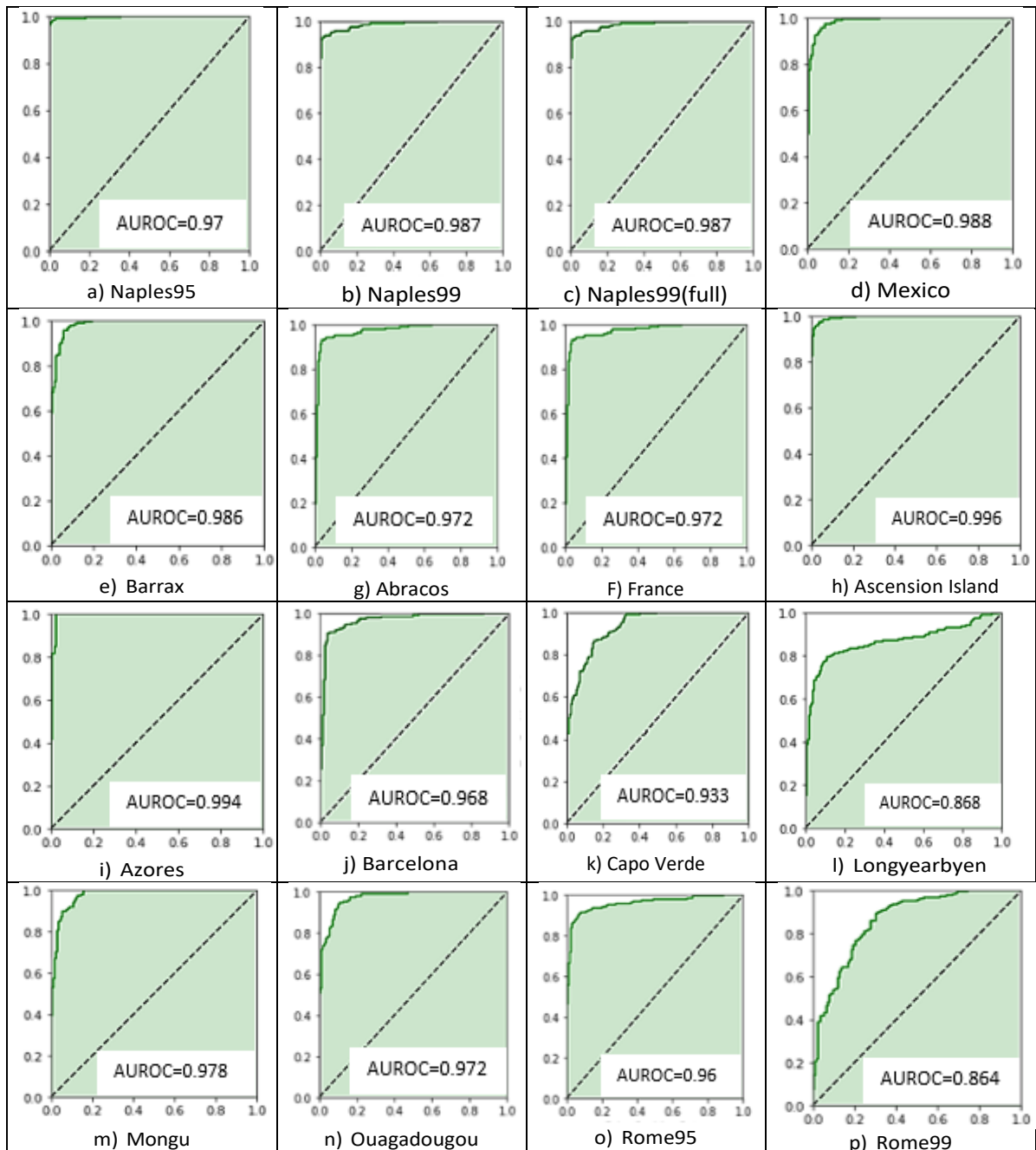
Figure 2: AUROC of Applying SVM-QA on 16 Datasets

Note: horizontal axis represents false positive rate, and vertical axis represents true positive rate.

Overall, our findings show that SVM-QA provides better accuracy. When compared to both the best results reported on HyperLabelMe and from our own results, SVM-QA performs consistently in classification accuracy, outperforming the reported 7 best machine learning algorithms in 10 out of 16 datasets and comes very close in the remaining datasets.

5. Discussion

Remote sensing data provides information to detect and monitor activities and changes in a geographical area with broad applications in a range of fields [11]. It plays an important role in scientific research areas such as astronomy, oceanic sciences, and atmosphere sciences, as well as commercial applications such as business location selection [50], geolocation-based social networks [51], smart waste collection systems [52], and also social well-being initiatives like poverty alleviation [53].

The rapid growth of remote sensing data collected from various sources has made it imperative to develop and deploy advanced and robust data processing tools. As a result, machine learning and deep learning have been widely used in the classification of remote sensing data. However, the performance of these tools varies depending on the data's characteristics. In addition, the increasing demand for computing power to develop advanced tools poses a bottleneck for classical machine learning. With quantum computing emerging as a recent technological
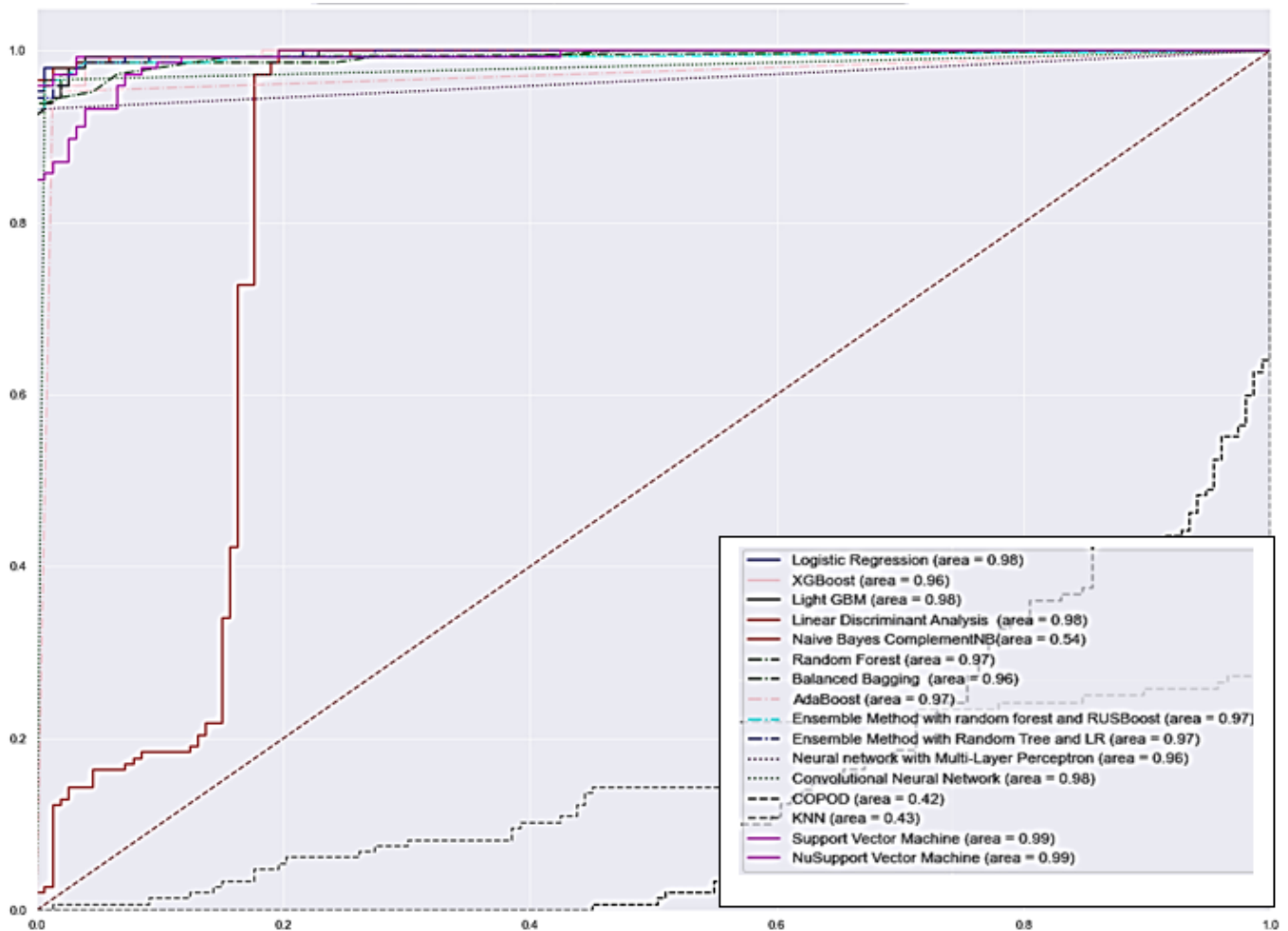
Figure 3: AUROC Curve of Applying 16 Machine Learning Algorithms on Dataset Naples95

Note: horizontal axis represents false positive rate, and vertical axis represents true positive rate.

breakthrough, offering capabilities for solving computationally impossible complex problems and scaling faster than traditional computing, we are motivated to investigate its potential to overcome the classical machine learning bottleneck in remote sensing image data field.

This study explores how Support Vector Machine, a popular supervised machine learning algorithm, performs when enhanced with quantum annealing. Using 16 labeled and harmonized image datasets from HyperLabelMe, we have compared the classification accuracy of SVM with quantum annealing enhancement to a standard SVM and two sets of top performing classical machine learning algorithms respectively. The results suggest that SVM-QA demonstrates promising accuracy in classification, outperforming most top performing machine learning algorithms that do not have the quantum computing enhancement. Because of quantum computing's capabilities to improve the performance of classical machine learning algorithms, there has been growing motivation to identify and expand quantum machine learning applications. However, literature on QML's applications in satellite image classification

remains somewhat limited. In [24], the authors report the application of quantum neural network in the satellite image classification and benchmarked it using low-resolution satellite data. Their finding suggests that QML approach produces better results. Studies that have applied other types of data also reach a similar conclusion. For example, in [17], the authors compare the performance of SVM trained on a D-Wave quantum annealer to SVMs used on conventional computers with both synthetic and real biology data, and they find that QML offers more generalizable solutions than the conventional SVM approach.

In this study, we have selected and applied the optimal γ (Gamma) value in the SVM-QA model implemented in the D-Wave computing environment. By comparing its classification results with those of over a dozen best classical machine learning algorithms on 16 HyperLabelMe datasets, our study provides more generalizable findings. This study contributes to the existing literature by offering broader and more in-depth understanding into remote sensing image binary classification. It expands the potential applications of

QML in satellite data classification and provides insights into achieving more accurate results.

6. Conclusion

This study has investigated the performance of binary classification of quantum enhanced machine learning algorithm compared to over a dozen classical machine learning algorithms across 16 satellite image datasets. Since support vector machine is a popular machine learning algorithm, we use quantum enhanced SVM in this study. The results suggest that quantum enhanced machine learning approach has often outperformed the classical machine learning approach.

Although SVM-QA has demonstrated superior performance compared to other machine learning algorithms, the evaluation is conducted in the context of harmonized hyperspectral remote sensing image datasets with small sample sizes and binary classification classes. We believe its potential with large datasets waits to be fully explored. We plan to evaluate SVM-QA's performance on much larger datasets with multiple classification classes and much larger images collected using different types of sensors, such as synthetic aperture radar (SAR) and light detection and ranging (LiDAR).

The development of quantum machine learning has made provision for the escalating development of computing, which will allow the accelerated progress of QML application to solve pressing and practical matters. Remote sensing is a field that requires multidisciplinary collaborations and inherently demands high computing power. We could leverage QML's computing capability in conducting real-time remote sensing environmental monitoring, timely disaster response, and efficient resource management. Although still in its infancy, quantum computing will definitely play an indispensable role in the near future.

Conflict of Interest

The authors declare no conflict of interest.

References

[1] S. Cuypers, A. Nascetti, and M. Vergauwen, "Land use and land cover mapping with vhr and multi-temporal sentinel-2 imagery, " *Remote Sensing*, vol. 15, 2501, 2023, doi:10.3390/rs15102501.

[2] M. Breunig, P.E. Bradley, M.W. Jahn, P.V. Kuper, N. Mazroob, N. R¨osch, M. Al-Doori, E. Stefanakis, and M. Jadidi, "Geospatial data management research: Progress and future directions," *ISPRS International Journal of Geo-Information*, vol. 9, no. 95, 2020, doi:10.3390/ijgi9020095.

[3] M. Aslam, M.T. Ali, S. Nawaz, S. Shahzadi, and M.A. Fazal, "Classification of Rethinking Hyperspectral Images using 2D and 3D CNN with Channel and Spatial Attention: A Review", *Journal of Engineering Research and Sciences*, vol. 2, no. 4, pp. 1-9, 2023, doi: 10.55708/js0204003.

[4] Y.D. Pyanylo, V. Sobko, H. Pyanylo, and O. Pyanylo, " Orthogonal Polynomials in the Problems of Digital Information Processing", *Journal of Engineering Research and Sciences*, vol. 2, no. 5, 2023, doi: 10.55708/js0205001

[5] Y. Shi, D. Campbell, X. Yu, and H. Li, "Geometry-guided street-view panorama synthesis from satellite imagery," *IEEE Transactions on Pattern Analysis and Machine Intelligence*, vol. 44, pp. 10009-10022, 2022, doi:10.1109/TPAMI.2022.3140750.

[6] P. Weber and D. Chapman, "Location intelligence: An innovative approach to business location decision-making," *Transactions in GIS*, vol. 15, 2011.

[7] U. Bayr, "Quantifying historical landscape change with repeat photography: An accuracy assessment of geospatial data obtained through monoplotting," *International Journal of Geographical Information Science*, vol. 35, pp. 2026–2046, 2021, doi:10.1080/13658816.2021.1871910.

[8] M. Riedel., G. Cavallaro, and J. A. Benediktsson, "Practice and experience in using parallel and scalable machine learning in remote sensing from hpc over cloud to quantum computing," in 2021 IEEE International Geoscience and Remote Sensing Symposium IGARSS, Brussels, 2021, pp. 1571–1574, doi:10.1109/IGARSS47720.2021.9554656.

[9] A. Sebastianelli, D. A. Zaidenberg, D. Spiller, B.L, Saux, and S.L.Ullo, "On circuitbased hybrid quantum neural networks for remote sensing imagery classification," *IEEE Journal of Selected Topics in Applied Earth Observations and Remote Sensing*, vol. 15, pp. 565–580, 2021, doi:10.1109/JSTARS.2021.3134785.

[10] D.A. Zaidenberg, A. Sebastianelli, D. Spiller, and S.L. Ullo, "*Advantages and bottlenecks of quantum machine learning for remote sensing,*" in 2021 IEEE International Geoscience and Remote Sensing Symposium IGARSS, Brussels, pp. 5680–5683, 2021, doi:10.1109/IGARSS47720.2021.9553133.

[11] G. Cheng, X. Xie, J. Han, L. Guo, and G. Xia, "Remote sensing image scene classification meets deep learning: Challenges, methods, benchmarks, and opportunities," *IEEE Journal of Selected Topics in Applied Earth Observations and Remote Sensing*, vol. 13, pp. 3735–3756, 2020.

[12] S. Crommelinck, M. Koeva, M.Y. Yang, and G. Vosselman, "Application of Deep Learning for Delineation of Visible Cadastral Boundaries from Remote Sensing Imagery," *Remote Sensing*, vol. 11, 2505, 2019, doi: 10.3390/rs11212505.

[13] S. Fujita and M. Hatayama, "Estimation method for roof-damaged buildings from aero-photo images during earthquakes using deep learning," *Information Systems Frontiers*, vol. 25, pp. 351–363, 2021, doi:10.1007/s10796-021-10124-w.

[14] A.E. Maxwell, T.A. Warner, and F. Fang, "Implementation of machine-learning classification in remote sensing: An applied review," *International Journal of Remote Sensing*, vol. 39, pp. 2784–2817, 2018, doi:10.1080/01431161.2018.1433343.

[15] R. L. Lawrence and C.J. Moran, "The americaview classification methods accuracy comparison project: A rigorous approach for model selection," *Remote Sensing of Environment*, vol. 170, pp. 115–120, 2015, doi:https://api.semanticscholar.org/CorpusID:43784543.

[16] J. Mu˜noz-Mar´ı, E. Izquierdo-Verdiguier, M. Campos-Taberner, A. P´erez-Suay, L. G´omez-Chova, G. Mateo-Garc´ıa, A.B. Ruescas, V. Laparra, J.A. Padron, J. Amor´os-L´opez, and G. Camps-Valls, "Hyperlabelme: A web platform for benchmarking remote-sensing image classifiers," *IEEE Geoscience and Remote Sensing Magazine*, vol. 5, pp. 79–85, 2017, doi:10.1109/MGRS.2017.2762476.

[17] D. Willsch, M. Willsch, H. De Raedt, and K. Michielsen, "Support vector machines on the d-wave quantum annealer," *Computer*

Physics Communications, vol. 248, 107006, 2020, doi:10.1016/j.cpc.2019.107006

[18] V. N. Vapnik, The nature of statistical learning theory. In Statistics for Engineering and Information Science, 2000.

[19] C. Venkatesan, P. Karthigaikumar, A. Paul, S. Satheeskumaran, and R. Kumar, "Ecg signal preprocessing and svm classifier-based abnormality detection in remote healthcare applications," *IEEE Access,* vol. 6, pp. 9767–9773, 2018, doi:10.1109/ACCESS.2018.2794346.

[20] H. Cheng, Y. Liu, Y, D. Huang, and B. Liu, "Optimized forecast components-svm based fault diagnosis with applications for wastewater treatment," *IEEE Access*, vol. 7, pp. 128534–128543, 2019, doi:10.1109/ACCESS.2019.2939289.

[21] K.S. Sahoo, B.K. Tripathy, K. Naik, S. Ramasubbareddy, B. Balusamy, M. Khari, and D. Burgos, "An evolutionary svm model for ddos attack detection in software defined networks," *IEEE Access*, vol. 8, pp. 132502–132513, 2020, doi:10.1109/ACCESS.2020.3009733.

[22] C.K.I. Williams and M.W. Seeger, "Using the nyström method to speed up kernel machines," In NIPS, 2000.

[23] A. Delilbasic, G. Cavallaro, M. Willsch, F. Melgani, M. Riedel, and K. Michielsen, "Quantum support vector machine algorithms for remote sensing data classification," in 2021 IEEE International Geoscience and Remote Sensing Symposium IGARSS, pp. 2608–2611, 2021, doi:10.1109/IGARSS47720.2021.9554802.

[24] M.P. Henderson, J. Gallina, and M. Brett, "Methods for accelerating geospatial data processing using quantum computers," *Quantum Machine Intelligence,* vol. 3, pp. 1–9, 2020, doi:10.1007/s42484-020-00034-6.

[25] P. Date, D. Arthur, and L. Pusey-Nazzaro, "Qubo formulations for trainingmachine learning models," *Scientific Reports,* vol. 11, 2021, doi:10.1038/s41598-021-89461-4.

[26] Kuhn, H., A, W.T.: Nonlinear programming. In: 2nd Berkeley Symposium, pp.481–492, 1951.

[27] A. Lucas, "Ising formulations of many np problems," *Frontiers in physics*, vol. 2, no. 5, 2014, doi:10.3389/fphy.2014.00005.

[28] S. Otgonbaatar and M. Datcu, "Natural embedding of the stokes parameters of polarimetric synthetic aperture radar images in a gate-based quantum computer," *IEEE Transactions on Geoscience and Remote Sensing*, vol. 60, pp. 1–8, 2022, doi:10.1109/TGRS.2021.3110056.

[29] V.N. Smelyanskiy, E.G. Rieffel, S. Knysh, C.P. Williams, M.W. Johnson, M.C. Thom, W.G. Macready, and K.L. Pudenz, "A near-term quantum computing approach for hard computational problems in space exploration," *arXiv: Quantum Physics,* 2012, doi:10.48550/arXiv.1204.2821.

[30] I., Guyon, J. Weston, S.D. Barnhill, and V.N. Vapnik, "Gene selection for cancer classification using support vector machines," *Machine Learning,* vol. 46, pp. 389–422, 2004. doi:10.1023/A:1012487302797.

[31] S.W. Bailey, D. Otte, P.C. DiLorenzo, and J.F. O'Brien, "Fast and deep deformation approximations," *ACM Transactions on Graphics (TOG),* vol. 37, pp. 1–12, 2018, doi:10.1145/3197517.3201300.

[32] N.S. Altman, "An introduction to kernel and nearest-neighbor nonparametric regression," *The American Statistician,* vol. 46, pp. 175–185, 1992, doi:10.2307/2685209.

[33] L. Breiman, J..H. Friedman, R. A. Olshen, and C.J. Stone, "Regression Trees," in Classificationand regression trees, New York, USA, Routledge, 1984, chapter8, doi:10.1201/9781315139470.

[34] Y. Freund and R.E. Schapire, "A decision-theoretic generalization of on-line learning and an application to boosting," *Journal of computer and system sciences*, vol. 55, no. 1, pp. 119–139, 1997, doi:10.1006/jcss.1997.1504

[35] A. Lazarevic and V. Kumar, "Feature bagging for outlier detection," In Proceedings of the Eleventh ACM SIGKDD International Conference on Knowledge Discovery in Data Mining, 2005, doi:10.1145/1081870.1081891.

[36] J.D. Rnnie, L. Shih, J. Teevan, and D.R. Karger, "Tackling the poor assumptions of naive bayes text classifiers," In Proceedings of the 20th International Conference on Machine Learning (ICML-03), pp. 616–623 2003.

[37] A.G. Howard, M. Zhu, B. Chen, D. Kalenichenko, W. Wang, T. Weyand, M. Andreetto, and H. & Adam, "MobileNets: Efficient Convolutional Neural Networks for Mobile Vision Applications," 2017, *ArXiv*, abs/1704.04861.

[38] Z. Li, Y. Zhao, N. Botta, C. Ionescu, and X. Hu, "Copod: Copula-based outlier detection," In Proceedings of IEEE International Conference on Data Mining (ICDM), pp. 1118–1123, 2020.

[39] M. Pal, "Random forest classifier for remote sensing classification," *International Journal of Remote Sensing*, vol. 26, pp. 217–222, 2005 doi:10.1080/01431160412331269698.

[40] C. Seiffert, T.M. Khoshgoftaar, J.V. Hulse, and A. Napolitano, "Rusboost: A hybrid approach to alleviating class imbalance," *IEEE transactions on systems, man, and cybernetics-part A: systems and humans*, 40, pp. 185–197, 1997. doi:10.1109/TSMCA.2009.2029559.

[41] G. Huang, Q. Y. Zhu, and C.K. Siew, "Extreme learning machine: Theory and applications," *Neurocomputing,* vol. 70, pp. 489–501, 2006, doi:10.1016/j.neucom.2005.12.126.

[42] T. Chen and C. Guestrin, "Xgboost: A scalable tree boosting system," in Proceedings of the 22nd ACM SIGKDD International Conference on Knowledge Discovery and Data Mining, 2016, doi:10.1145/2939672.2939785

[43] A.J. Izenman, "Linear Discriminant Analysis," In: *Modern Multivariate Statistical Techniques*, Springer Texts in Statistics, Springer, 2013, New York, NY, doi:10.1007/978-0-387-78189-1_8.

[44] G. Ke, Q. Meng, T. Finley, T. Wang, W. Chen, W. Ma, Q. Ye, and T.Y. Liu, "Lightgbm: A highly efficient gradient boosting decision tree," in Proceedings of the 31st International Conference on Neural Information Processing Systems, Long Beach, pp. 3149–3157, 2017.

[45] W. Chen, Y. Chen, Y. Mao, and B.L. Guo, "Density-based logistic regression," in Proceedings of the 19th ACM SIGKDD International Conference on Knowledge Discovery and Data Mining, 2013, doi:10.1145/2487575.2487583

[46] S. Lee and J.Y. Choeh, "Predicting the helpfulness of online reviews using multilayer perceptron neural networks," *Expert Systems with Applications*, vol. 41, pp. 3041–3046, 2014, doi:10.1016/j.eswa.2013.10.034.

[47] C.J. Burges, "A Tutorial on Support Vector Machines for Pattern Recognition," *Data Mining and Knowledge Discovery*, vol. 2, pp. 121-167. 1998.

[48] P. H. Chen, C.J. Lin, and B. Schölkopf, "A tutorial on v-support vector machines", *Applied Stochastic Models in Business and Industry*, vol. 21, pp. 111–136, 1997, doi:10.1002/asmb.537.

[49] J.A. Hanley and B.J. McNeil, "The meaning and use of the area under a receiver operating characteristic (roc) curve," *Radiology*, vol.143, no. 1, pp. 29–36, 1982, doi:10.1023/A:1012487302797.

[50] Y. Xu, Y. Shen, Y. Zhu and J. Yu, "Ar2net: An attentive neural approach for business location selection with satellite data and urban data," *ACM Transactions on Knowledge Discovery from Data*, vol. 14, no. 2, 20, pp. 1-28, 2020, doi:10.1145/3372406.

[51] A. Likhyani and S.J., P, D. Bedathur, "Location-specific influence quantification in location-based social networks," *ACM Transactions on Intelligent Systems and Technology (TIST)*, vol. 10, pp. 1–28, 2019. doi:10.1145/3300199.

[52] J.M. Gutierrez, M. Jensen, M. Henius, and T.M. Riaz, "Smart waste collection system based on location intelligence," vol. 61, pp. 120–127, 2015, doi:10.1016/j.procs.2015.09.170.

[53] N. Jean, M., Burke, S.M. Xie, W.M. Davis, D. Lobell, and S. Ermon, "Combining satellite imagery and machine learning to predict poverty," *Science*, vol. 353, pp. 790–794, 2016, doi:10.1126/science.aaf7894.

YI LIU has received her Ph.D. in Computer Sciences from the University of Mississippi, in 2005. Her research interests include software frameworks, software design patterns, software engineering aspects of cybersecurity, and geospatial data science. She received NIH and NASA grants for her research on using remote sensing datasets to detect and forecast outbreaks of mosquito-borne diseases.
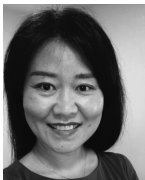
WENDY WANG has completed his PhD in Information Systems from the University of Mississippi, in 2002. She has published book chapters and manuscripts in the Journal of the American Society for Information Science and Technology, International Journal of Enterprise Information Systems, and Journal of Decision Systems. Her research interest includes IT application and their behavioral and social impact.

HAIBO WANG received his Ph.D. degree in business administration from The University of Mississippi in 2004. He is currently a Radcliff Killam Distinguished Professor in decision science and operations research with Texas A&M International University, USA. He has publications in IEEE Transactions journals, Omega, EJOR, and other major OR journals. His current research interests include analytics of big data in logistics, public transportation planning, information security, and health care.

BAHRAM ALIDAEE received his Ph.D. degree in mathematical sciences from the University of Texas at Arlington, in 1988. He has published in Management Science, Production and Operations Management, Transportation Science, various IEEE Transactions, and other major operations journals. His research interest includes applied management science interests of businesses